Public Transport Electrification: Lessons from a Pioneer*

Felipe González Hugo E. Silva

Abstract

Cities worldwide are committing to zero-emission bus fleets. We evaluate a pioneer: Santiago, Chile, whose electric bus fleet is the largest outside China. The timing of electrification across routes was set by concession expirations fixed years before electrification entered the policy agenda. Using this variation, we find that fully electrifying a route raises ridership by 4–6 percent without changing operating speed; that $PM_{2.5}$ and NO_x concentrations fall near electrified service; that accident rates fall by 20 percent; and that peak-hour noise falls modestly. Valued at official social prices, these gains amount to USD 215 to 668 million per year in 2025, depending on how avoided deaths are valued, between one-sixth and one-half of the system's annual public subsidy. Because tenders spread the capital premium over time and offset it with lower operating costs, the gains came at approximately no additional cost.

Keywords: electric buses; public transport; air pollution; traffic safety; procurement.
JEL codes: H23, H57, O33, Q53, R41, R48.

---

*This version: July 2026. González: King's Business School, King's College London; Centre for Economic Policy Research; and Instituto de Economía, Pontificia Universidad Católica de Chile. Silva: Instituto de Economía and Departamento de Ingeniería de Transporte y Logística, Pontificia Universidad Católica de Chile; Center for Advanced Transportation, Logistics, and Economic Competitiveness (CATLEC) (ANID/CIN 250061); and Millennium Nucleus in Just Transport (ANID/NCS2025 71). We gratefully acknowledge financial support from Center for Advanced Transportation, Logistics, and Economic Competitiveness (CATLEC). We thank people working in DTPM for their help with the data and useful comments. We also thank Juan Carlos Muñoz, Nathaly Rivera, and Luis Rizzi for comments and suggestions. We received excellent research assistance from Francisca Adasme. Contact email: `felipe.gonzalez@kcl.ac.uk`.

1 Introduction

Climate change has moved the transition to zero-emission technologies to the center of public policy, and a growing literature evaluates the welfare effects of the taxes and subsidies deployed to accelerate it (Acemoglu et al., 2016; Feger et al., 2022; Hahn et al., 2026). The case for this transition rests only partly on carbon: burning fossil fuels also degrades local air quality, and quasi-experimental evidence shows that even short-lived increases in exposure raise mortality, medical spending, and hospital admissions (Schlenker and Walker, 2016; Deryugina et al., 2019). Public buses have become a leading margin of adjustment in this transition, and commitments now span regions across the world. For example, the European Union requires all new urban buses to be zero-emission by 2035, and London has committed to a fully zero-emission fleet by 2034; São Paulo must eliminate fossil CO_2 emissions from its bus fleet by 2038; Jakarta plans to electrify its entire 10,000-bus fleet by 2030; and the largest transit agencies in the United States have committed to fully zero-emission fleets: New York and Chicago by 2040, and Seattle's King County Metro by 2035.[1]

Santiago de Chile offers an unusually good setting to provide that evidence. The city moved early and at scale: its electric bus fleet is the largest of any city outside China, and electric buses account for half of the operating fleet (DTPM, 2025). The setting also offers administrative data of rare quality: the universe of bus trips, georeferenced and linked to ridership; networks of air- and noise-pollution monitors; and microdata on respiratory emergency visits and school absenteeism. Each trip record includes the bus license plate, which we match to the fleet registry identifying every vehicle's engine technology, so electrification is measured from realized operations, bus by bus and trip by trip, rather than from fleet stocks. Finally, the rollout embeds credible exogenous variation. The timing of electrification across routes was determined by the expiration of concessions signed in 2007 and renegotiated in 2011, years before electrification entered the policy agenda, so deployment timing is unrelated to the pollution burden or the health profile of the areas served (Gómez-Lobo, 2025; Muñoz et al., 2014).

We use these data and this variation to trace the welfare effect of electrification through the margins it can move. Fleet replacement changes the attributes and ridership of bus service, the externalities that bus operations impose on nearby places, and the resource cost

[1]See European Parliament and Council of the EU (2024); Transport for London (2023); Município de São Paulo (2018); The Jakarta Post (2020); Metropolitan Transportation Authority (2024); Chicago Transit Authority (2022); King County Metro Transit (2022) for details.

of provision. We estimate each margin from a common design. We compare the same route or location before and after its service becomes more electric, relative to other units observed on the same day. For the external outcomes we hold total bus activity fixed, so the estimates isolate a change in fleet composition, which we call a replacement effect, rather than a change in the amount of service. Identification comes from the staggered expiration of operating contracts, so a route's electrification timing is unrelated to its pollution, noise, accident, or health profile. Section 3 states this framework and writes the welfare effect as a sum of the components we estimate.

The results follow this chain. First, electrification changed how buses are used, but not how fast they move. As a route's electric share rises, operators deploy more vehicles, passenger usage rises in every period, and ridership increases by about 4 percent in peak hours and 6 percent off-peak and on weekends. Average operating speed does not change, and the estimates are precise zeros. The passenger response therefore does not run through faster trips. It reflects the broader upgrade in service that accompanies fleet renewal, such as newer, quieter, and more comfortable vehicles. We read our estimates as the effect of the electrification package as it is actually implemented, not of the drivetrain in isolation.

Second, electrification reduced the local externalities of bus travel. The clearest effect is on air pollution. At a monitoring location with average nearby bus activity, full electrification lowers daily $PM_{2.5}$ by about 6.7 $\mu g/m^3$ and reduces nitrogen oxides, holding total bus activity fixed. Traffic accidents fall as well: a fully electrified route has about 20 percent fewer accidents and injuries per kilometer than a comparable diesel route, a result that is stable across specifications. Ambient noise falls near the busiest corridors during peak hours, by about 1.4 dB(A) within 50 meters, though this estimate is less robust than the other two. Each effect is identified from within-location or within-route variation, net of citywide daily shocks, so it reflects the change in fleet composition rather than the amount of service.

Third, these environmental gains are harder to detect in downstream health and schooling. Respiratory emergency-room visits fall after nearby service becomes highly electric, but the decline is imprecise and is matched by a similar fall in non-respiratory visits, so it is not specific to respiratory causes. School absenteeism shows no measurable response. These muted results are what the size of the pollution reductions implies. Mapped through published concentration–response estimates, the expected changes in emergency visits and absences are small relative to the month-to-month variation in these outcomes, and our health and schooling data are measured at coarser time and spatial scales than the localized

daily pollution changes we estimate. We read this evidence as bounding the downstream response and disciplining the health valuation, not as a clean test.

Finally, we value these effects at the official social prices of the Chilean public-investment system and weigh them against costs. On the cost side, the re-tenders electrified the fleet at approximately no additional resource cost: the higher capital cost of electric buses was offset by lower energy and maintenance costs, and the transport authority reports that the 2023 and 2025 tenders reduced annual system payments. Because the incremental resource cost is near zero, the sign and rough magnitude of the welfare effect are set by the externality and ridership responses we estimate.

Among these, the mortality gains from lower particulate exposure are the largest benefit, with smaller contributions from fewer accidents, less noise, avoided carbon, and higher fare revenue. Because the mortality valuation drives the total, we report it under two conventions throughout. In 2025, with 42 percent of bus service electric, the benefits amount to USD 668 million per year valuing avoided deaths at the official statistical-life value, and USD 215 million under a life-years valuation. For scale, the annual public subsidy that finances the system, buses, Metro, and commuter rail combined, is about USD 1.3 billion: the realized gains equal between one-sixth and one-half of it. Section 7 reports the full valuation.

Our first contribution is to the economic evidence on green-transition policy. Most of this evidence concerns instruments that operate through private adoption decisions: net energy metering for rooftop solar (Bollinger et al., 2025), public investment in electric-vehicle charging infrastructure (Arkolakis et al., 2025), and the electrification of residential heating (Davis, 2024, 2025). A recurring lesson is that the returns to these instruments hinge on margins the government does not control: how households discount future savings (Bollinger et al., 2025), whether they use the technology at all (Hanna et al., 2016), and the pricing and carbon content of the electricity behind it (Borenstein and Bushnell, 2022; Gillingham et al., 2025). Public bus fleets differ on exactly this margin: the state is the adopter, and the new technology directly replaces diesel buses, among the dirtiest vehicles operating in dense urban corridors. We complement welfare evaluations of green-transition policies (Hahn et al., 2026) with causal evidence on the realized effects of one of the largest state-led electrification programs to date.

Our second contribution is to the literature on technology adoption by the state (Acemoglu et al., 2016). A recent experimental literature studies governments adopting information technologies to improve their own operations: biometric payments and identity verification

in welfare programs (Muralidharan et al., 2016, 2025), e-invoicing in workfare (Banerjee et al., 2020), electronic procurement (Lewis-Faupel et al., 2016), electronic tax filing (Okunogbe and Pouliquen, 2022), and automated environmental monitoring (Greenstone et al., 2022; Assunção et al., 2023). These technologies work by generating information that mitigates agency problems inside the state, and their returns hinge on whether the government acts on that information (Dhaliwal and Hanna, 2017; Muralidharan et al., 2025). The technology we study is of a different kind: a production technology embedded in service delivery, whose returns (cleaner air, fewer accidents, more attractive service) accrue directly to citizens rather than through improved monitoring or enforcement. In Santiago, adoption also ran through competitive procurement, but the object procured was the technology itself. Our evidence documents what this form of state technology adoption delivers, a margin on which systematic evidence remains scarce.

We also contribute to transport economics, and in particular to the literature on policies that reduce the externalities of urban travel. First-best pricing of vehicle use at marginal external cost (Parry et al., 2007) remains politically and technologically difficult, so cities rely on a menu of second-best instruments: transit subsidies (Parry and Small, 2009; Basso and Silva, 2014), bus priority infrastructure (Basso and Silva, 2014; González and Silva, 2025), lane exemptions that reward cleaner vehicles (Bento et al., 2014), and driving restrictions targeting older vintages, pioneered by Santiago in 1992 (Barahona et al., 2020), with recent work evaluating such policies in general equilibrium (Barwick et al., 2024). Each instrument buys its gains on one margin at a cost on another: subsidies strain public budgets (Parry and Small, 2009), uniform restrictions push households toward additional, dirtier cars (Barahona et al., 2020), and cleaner engines lose potency at congested speeds (Waxman et al., 2024). Judged against this menu, fleet electrification performs unusually well: pollution and accidents fall along electrified routes while ridership rises, with operating speeds unchanged. Locating a policy with these properties in the second-best toolkit is directly relevant for the growing number of cities committed to zero-emission fleets.

2 Context

Santiago is the capital of Chile and its largest metropolitan area, with a population of about seven million. The city sits in a basin between the coastal mountain range and the Andes, and a persistent subsidence inversion limits vertical mixing. This geography traps

local emissions and has made air pollution a first-order policy problem for decades (Barraza et al., 2017). Despite sustained abatement policies since 1990, annual $PM_{2.5}$ concentrations remain well above the WHO guideline and hover around the Chilean standard (Barraza et al., 2017; IQAir, 2025); panel (c) of Figure 1 places these concentrations in international perspective. Santiago also has one of the world's longest-running $PM_{2.5}$ monitoring networks, with continuous records since 1989.

2.1 Transport, pollution, and health

Urban air pollution comes mostly from combustion, and in Santiago transport plays a leading role. The official emissions inventory attributes 20% of the Metropolitan Region's $PM_{2.5}$ emissions and 60% of its NO_x emissions to transport (MMA, 2017). Emissions, however, are not the same as exposure: wood burning is concentrated in winter and in peripheral areas, while vehicles emit at street level across the city throughout the year. Source-apportionment estimates based on 15 years of filter samples in central Santiago attribute 37% of ambient $PM_{2.5}$ to motor vehicles (Barraza et al., 2017).[2] As panel (d) of Figure 1 shows using data up to 2012, this share was among the highest in the world: it matched the population-weighted average of India and stands well above the world average of 25% (Karagulian et al., 2015).

Within the transport sector, diesel buses are a disproportionate source of harmful local pollutants. They account for about a quarter of the black carbon emitted by the transport sector, and where soot-free engines are not required, a diesel bus can release more than 250 times the black carbon of a gasoline car over the same distance (Climate and Clean Air Coalition, 2017). In much of Latin America the bus fleet still meets only Euro III standards or worse, and until recently only Mexico City and Santiago required Euro VI engines for new buses (Miller et al., 2017; Fun Sang Cepeda et al., 2025). Santiago was no exception before the fleet renewal we study: 82% of its roughly 6,500 buses were Euro III (Climate and Clean Air Coalition, 2017). Moreover, bus emissions are released at street level along dense corridors, so exposure is concentrated precisely where people live, walk, and wait.

A large body of evidence links localized traffic pollution to health. Currie and Walker (2011) find that electronic tolling, by cutting congestion and idling at toll plazas, reduced

[2]The full apportionment is 37% motor vehicles, 19% industrial sources, 14% copper smelters, 12% residential wood burning, 10% coastal sources, and 3% urban dust, with wood burning rising to roughly 31% in the cold season (Barraza et al., 2017). On the emissions side, the inventory attributes 39% of $PM_{2.5}$ to residential wood burning, 20% to off-road machinery, and 15% to industry (MMA, 2017).

prematurity by 10.8% and low birth weight by 11.8% among mothers living within 2 km of a plaza. Schlenker and Walker (2016) show that daily variation in airport congestion raises respiratory and heart-related hospital admissions within 10 km of California airports. For Chile, Dardati et al. (2024) estimate that a one-day increase of 1 $\mu g/m^3$ in $PM_{2.5}$ raises respiratory emergency-room visits by 0.36%. Replacing diesel buses with zero-emission vehicles can therefore produce health benefits that are large and highly localized, which is the hypothesis we take to the data.

2.2 Bus fleet electrification

Electric buses have become a central tool for decarbonizing urban transport. Their fixed routes, central depots, and shared charging infrastructure make electrification easier to manage than for private vehicles (Avenali et al., 2024). Adoption has accelerated but remains uneven: more than 90% of the world's roughly 780,000 electric buses operate in China, and large fleets outside China remain uncommon (Jaeger, 2025).[3] The main obstacle is cost: electric buses carry higher capital costs for batteries and charging, and operators resist adoption without direct public support (Avenali et al., 2023; Giagnorio et al., 2024). Panels (a) and (b) of Figure 1 put Santiago in this global context: it operates the largest electric bus fleet of any city outside China, and close to half of its fleet is electric, among the highest shares outside China (DTPM, 2025).

Santiago's bus system has been the main testing ground for Chile's climate commitments, which include an emissions peak in 2025, carbon neutrality by 2050, and, for public transport, zero-emission requirements for all new urban fleet additions by 2035 and fully zero-emission operation by 2040.[4] In 2019, Santiago became one of the first cities in the world to require Euro VI (or EPA 2010) engines for every new bus, a standard that mandates particulate filters and cuts PM emissions by about 90% relative to Euro V (Climate and Clean Air

[3]In Europe, the electric bus fleet grew from about 1,650 in 2018 to more than 9,500 in 2022, and the electric share of new bus sales rose from 2.5% to 10% (European Alternative Fuels Observatory, 2022); a European mandate requires all new urban buses to be zero-emission by 2035 (European Parliament and Council of the EU, 2024).

[4]Chile pledged in 2015 to reduce the emissions intensity of GDP by 30% by 2030 relative to 2007 and, as host of COP25 in 2020, set a maximum emissions budget of 1,100 million tonnes of CO_2-equivalent for 2020–2030. The targets rest on state policies sustained across administrations and led jointly by the Ministries of Energy, Environment, and Transport, including the 2050 Energy Policy, the National Electromobility Strategy, the Energy Efficiency Law, the Energy Storage and Electromobility Law, and the sector's Sustainable Mobility Policy.

Coalition, 2017). Electrification started in parallel: the first electric buses arrived as pilots in 2017, and the first large batch of 100 vehicles entered service in late 2018 (DTPM, 2025). Figure 2 documents this transformation: by late 2025, electric buses accounted for close to half of the operating fleet (panel a) and of daily bus trips (panel b).

2.3 Contracts and rollout

The institutional origins of the rollout date back two decades. Gómez-Lobo (2025) documents how Santiago's public transport system was overhauled almost overnight on February 10, 2007. This reform, known as Transantiago, simultaneously restructured the route network, the fare collection technology, the bus fleet, and the contracts governing operators. The reform precipitated a combined mobility and political crisis, and the State's subsequent effort to improve the system cost roughly 0.25% of GDP (Gómez-Lobo, 2025).

The original 2007 concessions assigned markedly different terms to feeder (*alimentador*) and trunk (*troncal*) services: feeder contracts ran for six years, expiring in 2012, while trunk contracts ran for thirteen years. These concessions were renegotiated during 2011 under the legal framework of Law 20.504 (Muñoz et al., 2014), whose central provision for our purposes governed how the Ministry of Transport could proceed once a concession was terminated early: re-tender, award a three-year direct contract, or award transitional eighteen-month contracts.[5] Some operators ran to the end of their original term, others accepted three-year direct contracts, and others entered successively renewed eighteen-month arrangements. Contract expirations therefore became staggered across operators and routes. Importantly, both the 2007 terms and the 2011 options were set well before fleet electrification entered the policy agenda, so the expiration schedule was fixed by institutional considerations unrelated to environmental or health objectives.

The link to electrification follows directly. When a contract reached its end, the corresponding routes were re-tendered, and the later tenders incorporated an electric fleet as a contractual requirement. The arrival of electric buses on a route was thus determined by *when* its incumbent contract happened to expire, rather than by the route's pollution burden or the health profile of the population it served. Figure A.1 in Section 5.1 illustrates the resulting

[5]The Ministry was required to designate a new concessionaire within eighteen months of the termination resolution becoming final, ordinarily through a new public tender. On grounds of public interest and service continuity, it could instead award service directly on a transitional basis, for up to three years or until the end of the original concession term, by decree jointly signed by the Ministers of Transport and Finance.

variation in timing and intensity across locations.

A final feature of the re-tenders matters for the welfare analysis. The new contracts separated fleet provision from operation and spread the capital cost of the electric fleet over the contract horizon. This capital premium was approximately offset by the lower energy and maintenance costs of electric operation: the transport authority reports operating-cost savings of 66 percent and maintenance savings of 44 percent for electric buses, and estimates that the 2023 and 2025 re-tenders reduced annual system payments (Directorio de Transporte Público Metropolitano, 2026). The fleet was therefore electrified without a material increase in the resource cost of providing service. We return to this feature in Section 3.

3 Framework and Empirical Design

Fleet electrification replaces one production technology of public transport with another, on a fixed route network and under a fare set citywide by the regulator. Its welfare consequences therefore run through a small number of margins. This section writes the welfare effect of electrification as a sum of interpretable components, defines the two estimands the paper recovers, and states once the empirical design and identifying assumption that all subsequent analyses share.

3.1 Welfare margins of fleet replacement

Consider a city that provides bus service over a fixed route network. Let K denote total bus-kilometers supplied per period and $s \in [0,1]$ the share of those kilometers operated with electric buses; electrification is an increase in s. The technology mix determines a vector of service attributes $q(s)$ (vehicle age and comfort, noise inside and outside the vehicle, passenger capacity per kilometer, reliability) and, given the regulated fare p, ridership $R(p,q)$. The mix also determines the quantities of externalities generated by bus operations, $X_j(s,K)$, where j indexes local air pollutants, ambient noise, traffic accidents, and carbon. Writing $C(s,K)$ for the resource cost of provision and φ_j for the marginal external damage of X_j in money terms, social welfare per period is

$$W(s) = \underbrace{CS\big(p,q(s)\big)}_{\text{rider surplus}} + \underbrace{p\,R\big(p,q(s)\big) - C(s,K)}_{\text{fare revenue net of resource costs}} - \underbrace{\sum_j \varphi_j\, X_j(s,K)}_{\text{external costs}}, \tag{1}$$

where CS is consumer surplus and transfers between the government and operators net out. Differentiating with respect to s, holding K fixed for clarity, the welfare effect of electrification is

$$\frac{dW}{ds} = \underbrace{\frac{\partial CS}{\partial q}\frac{dq}{ds} + p\,\frac{dR}{ds}}_{\text{transit-market effects}} - \underbrace{\frac{\partial C}{\partial s}}_{\text{resource costs}} - \underbrace{\sum_j \varphi_j \frac{dX_j}{ds}}_{\text{external effects}}. \tag{2}$$

The three terms collect the transit market, the resource cost of the technology switch (the procurement premium for vehicles and charging infrastructure, net of energy and maintenance savings), and the externalities of bus operations. In practice operators also adjust deployment along with technology, so q and even K are outcomes of the policy rather than parameters; this is why the empirical analysis treats the service margins as objects to be estimated, and why the externality designs must hold total bus activity fixed.

Equation (2) organizes the paper. Section 4 estimates the transit-market responses: how deployment, capacity, and speed (the attributes in q) and ridership R change when routes switch to electric operation. Section 5 estimates dX_j/ds for the three local externalities: air pollution (Section 5.1), traffic accidents (Section 5.2), and ambient noise (Section 5.3). Section 6 adds no separate welfare term: it asks whether the pollution reductions reappear downstream, in respiratory emergency visits and school absenteeism, at magnitudes consistent with published concentration–response relationships (Dardati et al., 2024; Chung et al., 2025), disciplining the pollution valuation rather than introducing a new margin.

Two components of Eq. (2) come from institutions and prices rather than from quasi-experimental variation. The first is the resource-cost term, which in Santiago's implementation is approximately zero because the re-tenders offset the capital premium of the electric fleet with lower energy and maintenance costs (Section 2.3). If the offset is exact, the sign of the welfare effect is determined entirely by the responses we estimate. The second is the carbon term, which is set by the emissions intensity of the national grid. Combining our estimates with damage valuations and grid data into a full welfare evaluation, in the spirit of Hahn et al. (2026), requires no further behavioral estimates; Section 7 performs this aggregation.

3.2 Two estimands

Because deployment responds to electrification, the paper distinguishes two estimands. The first is a *package effect*: the change in a route's outcomes when its service moves from fully

conventional to fully electric operation, as implemented. Electrification arrives as a bundle: new vehicles, different capacities and comfort, new charging and maintenance routines, and operator deployment decisions. No government replaces drivetrains while holding every other attribute of service fixed. The package effect is the policy-relevant object for the adoption decision, and it is the estimand for the transit-market outcomes in Section 4.

The second is a *replacement effect*: the change in outcomes at a fixed location when electric bus-kilometers replace conventional bus-kilometers nearby, holding total nearby bus activity constant. Externalities accrue to places, so the natural unit of analysis is a location exposed to the operations of many routes. The conditioning on total activity separates technology composition from service scale: because bus-kilometers themselves respond to electrification, a location-level regression without this control would confound cleaner buses with more or fewer buses. The replacement effect is the estimand for pollution, noise, accidents, and the downstream outcomes, and it is the object that corresponds to dX_j/ds in Eq. (2).

3.3 A common design

All analyses estimate variants of a single specification. Let u index the unit at which an outcome is measured, a route for market outcomes and accidents and a fixed location (air-quality or noise monitor, satellite grid cell, health center, or school) for the rest, and let t index time at the frequency the outcome is observed. We estimate

$$Y_{ut} = \beta\, Electric_{ut} + \gamma\, Total_{ut} + \alpha_u + \delta_t + \varepsilon_{ut}, \tag{3}$$

where $Electric_{ut}$ and $Total_{ut}$ measure the electric and total bus activity to which unit u is exposed at time t, and α_u and δ_t are unit and time fixed effects. The two estimands are versions of β. At the route level, the treatment is the electric share of bus-kilometers and β recovers the package effect. At the location level, the treatment is electric bus-kilometers with total bus-kilometers included as a control, and β recovers the replacement effect. Each section states the estimator it uses for this design (least squares, PPML for counts, or an event-window version). Unit fixed effects absorb permanent differences across units; time fixed effects absorb citywide shocks such as weather, fare changes, and aggregate pollution episodes.

Treatment exposure is built from the same administrative source throughout: the universe

of bus trips, matched to vehicle technology through license plates and to space through route geometries. For fixed locations, we draw buffers around each unit and allocate route-day bus-kilometers in proportion to the length of the route lying inside the buffer; Figure 3 maps the network together with the units of analysis. The buffer radius follows the spatial reach of the outcome rather than the availability of data: 5 km for pollution, which disperses over kilometers; 50 to 200 meters for noise, which attenuates within a few hundred meters; and intermediate radii for accidents, emergency centers, and schools, stated in each section.

Identification is the same in every design and comes from the contractual chronology described in Section 2.3: the timing and intensity of a route's electrification were governed by when its contract happened to expire, not by the pollution burden, noise environment, accident record, or health profile of the areas it serves. The identifying assumption, stated once for all designs, is that conditional on unit and time fixed effects (and, in replacement designs, on total nearby bus activity), the timing and intensity of electric-bus exposure are unrelated to unit-specific shocks to the outcome. Three features of the evidence support this assumption: the chronology was predetermined; event-study versions of Eq. (3) show no differential pre-trends where we can estimate them (Sections 5.2 and 6); and each design is probed against alternative exposure radii, unit-specific trends, and the influence of individual units, with the text flagging where the evidence weakens.

Two limits of the design are worth stating at the outset. First, the estimates are local and relative. Conventional buses displaced from an electrifying route may operate elsewhere until they are retired, so replacement effects capture the reallocation of bus emissions across space as well as their elimination; citywide aggregate effects, absorbed by the time fixed effects, are not identified by this design. Second, the design does not identify where new riders come from. If some substitute away from cars, the externality gains estimated here omit the associated reduction in car emissions, noise, and accident risk, making our external-effect estimates conservative on that margin.

4 Deployment and Service Response

This section estimates the package effect of electrification on the transit market, the first term of Eq. (2). Figure 2 documents the deployment margin at the level of the system: by late 2025, electric buses accounted for close to half of the operating fleet and of daily bus trips. We now follow that replacement at the level of individual routes and estimate how

the state and its contracted operators deployed the new technology (vehicles, kilometers, capacity, and speed) and how passengers responded.

4.1 Data construction

We construct a daily panel dataset that follows bus routes at the daily level between January 2022 and December 2025. The starting point is administrative information provided by the Ministry of Transportation for the universe of bus trips in Santiago. The data include, for each trip, the route identifier, the bus license plate, the date of operation, the start and end times, and the distance traveled, from which we infer average commercial speed. The route identifiers distinguish main routes and their variants, which allows us to keep the full operational structure of the network. Our final dataset covers approximately 1,300 routes.[6]

We combine the trip-level operating data with two additional administrative datasets. First, we use trip-level ridership data, also provided by the Ministry of Transportation, which records the number of passengers transported by each bus trip. Second, we merge the operating records with administrative information on the bus fleet using the license plate observed in the trip records. This fleet registry identifies the technology of each bus and allows us to identify electric buses. The bus fleet contains approximately 7,500 buses, but not all vehicles are operated every day and operators retain discretion over which buses to deploy across routes and times. Moreover, buses are not assigned exclusively to a single route: the same bus can operate on multiple routes within the same day. For this reason, we measure electrification using realized bus operations rather than fleet availability. In particular, for each route-day-time cell we compute the share of bus-kilometers operated by electric buses, defined as electric bus-kilometers divided by total bus-kilometers in that cell.

We aggregate the trip-level records to the route-day-time level, separately for workday peak hours, workday off-peak hours, and weekends. This aggregation preserves the margin at which the treatment varies while matching the level at which route-level outcomes are most naturally interpreted. For each route-day-time cell, we compute the number of distinct buses deployed, total bus-kilometers, passenger-capacity-kilometers, average operating speed, usage, and ridership. Bus-kilometers are the total kilometers traveled by all buses serving the route

[6]Peak and off-peak periods follow the official time categories of the Ministry of Transportation. Peak hours are 6:30–8:30 a.m. and 6:00–8:00 p.m. on workdays; off-peak hours are 9:30 a.m.–12:00 p.m., 2:30–5:00 p.m., and 9:30–10:30 p.m. on workdays. Weekend observations include all hours on Saturdays, Sundays, and holidays.

during the corresponding day and time period. Passenger-capacity-kilometers equal the passenger capacity of the vehicles, including both seated and standing capacity, multiplied by the kilometers traveled and divided by one million. Average speed is computed from the trip-level speeds and aggregated to the route-day-time cell. Usage is validations divided by available passenger capacity per trip, expressed as a percentage. Ridership is the total number of paying passengers transported in the cell.

This construction generates a panel in which the treatment is the realized intensity of electric-bus service on each route-day-time cell, rather than an indicator for whether a route has access to electric buses. The resulting variation reflects the gradual replacement of conventional bus service by electric bus service across routes and dates, while allowing for partial adoption within a route-day.

4.2 Specification

We estimate the effect of electric-bus adoption by comparing the same route before and after a larger share of its service is operated with electric buses. Let r denote a route, d a date, and h one of the time samples we study: workday peak hours, workday off-peak hours, or all weekend and holiday hours. We estimate the following equation separately by time sample:

$$Y_{rdh} = \beta ShareElectric_{rdh} + \phi_r + \theta_d + \varepsilon_{rdh}, \tag{4}$$

where Y_{rdh} is an outcome measured at the route-day-time level, $ShareElectric_{rdh} \in [0, 1]$ is the share of bus-kilometers in the cell operated by electric buses, ϕ_r are route fixed effects, and θ_d are date fixed effects. The coefficient of interest is β. Because the treatment is measured as a share, β corresponds to the change in the outcome when moving from a route-day-time cell with no electric-bus service to one in which all bus-kilometers are operated by electric buses. Estimating separately by time sample allows the effect to differ across periods with different congestion levels, operating constraints, and passenger demand.

Equation (4) is the route-level instance of the common design in Section 3.3: the treatment is the electric share of bus-kilometers, so β recovers the package effect, and identification comes from within-route changes in the electric share relative to other routes on the same date, with timing governed by the contractual chronology.

The outcomes, defined above, capture three margins: service supply (buses deployed, bus-kilometers, and passenger-capacity-kilometers), operations (average speed), and passenger

response (usage and ridership). All outcomes are estimated in levels except ridership, which enters in logarithms, so the ridership coefficient reads approximately as a percentage change.

We estimate Eq. (4) by weighted least squares for all outcomes except bus-kilometers. The weights are based on route size measured before treatment-induced changes in service supply: for each route, we compute average bus-kilometers during the first 60 days in which the route is observed in the corresponding estimation sample. This weighting scheme gives more influence to routes that account for a larger share of bus operations while avoiding contemporaneous weights that could themselves respond to electric-bus adoption. We do not use these weights when bus-kilometers is the dependent variable because the weight is constructed from the same source of variation that the regression is designed to explain. Robust standard errors are clustered at the route level, allowing for arbitrary serial correlation within routes over time.

4.3 Results

Table 1 presents the route-level estimates of Eq. (4). The coefficient on $ShareElectric_{rdh}$ should be interpreted as the effect of moving from no electric operation to full electric operation in the corresponding cell. The first three columns show that electric-bus adoption changes service supply in a non-mechanical way. In all periods, routes deploy more buses when a larger share of their kilometers is operated by electric vehicles. The increase is 1.7 buses during workday peak hours, 4.1 buses during workday off-peak hours, and 4.6 buses during weekends, and all three estimates are statistically significant. Relative to the average number of buses in each sample, these effects correspond to increases of 8 percent, 17 percent, and 10 percent, respectively. The effect on bus-kilometers is positive but smaller: peak-hour bus-kilometers increase by 13.9 kilometers, or 2.6 percent relative to the mean, while weekend bus-kilometers increase by 32.8 kilometers, also 2.6 percent relative to the mean. Both estimates are statistically significant, whereas the off-peak estimate is positive but not statistically different from zero. Thus, electric-bus adoption is associated with more vehicles being deployed and, in some periods, with more kilometers operated.

The capacity results in column 3 show that the increase in the number of buses does not translate into higher passenger capacity. During workday peak hours, electric-bus adoption reduces capacity-kilometers by 0.32 million, a decline of 22 percent relative to the mean. During weekends, the decline is 1.25 million capacity-kilometers, or 17 percent relative to the mean. Both estimates are statistically significant at the 1 percent level. During off-

peak hours, the point estimate is positive but small and statistically insignificant. These results imply that electric buses are not simply expanding service capacity. Instead, the adoption of electric buses appears to change the composition of service: routes operate with more vehicles, and sometimes more bus-kilometers, but with lower passenger capacity per kilometer in peak hours and on weekends. This pattern is consistent with electric buses replacing higher-capacity conventional buses, or with operators deploying electric vehicles differently across routes and times. It is useful to keep this finding in mind when interpreting the passenger response below, because any increase in ridership does not appear to be driven by a simple increase in passenger-capacity-kilometers.

Column 4 shows that average operating speed is essentially unaffected. The peak-hour and off-peak point estimates are both negative and close to zero: -0.09 km/h during peak hours and -0.08 km/h during off-peak hours. Relative to the sample means, these are changes of less than one half of one percent. During weekends, the estimate is exactly zero up to rounding. None of the speed estimates is statistically significant. This null result is economically informative. Electric buses may differ from conventional buses in acceleration, noise, and passenger comfort, but route-level commercial speed in Santiago is largely determined by traffic conditions, traffic lights, stops, dwell time, and road priority. The absence of a speed effect therefore suggests that electrification changes the fleet technology and some margins of service provision without meaningfully changing bus speed.

Columns 5 and 6 report passenger responses. Usage increases in all three samples. The coefficient is 0.31 during workday peak hours, 0.14 during workday off-peak hours, and 0.24 during weekends, with all three estimates statistically significant at the 1 percent level. Relative to the mean of the dependent variable, these effects are large: usage increases by 17 percent during peak hours, 9 percent during off-peak hours, and 41 percent during weekends.

Ridership also increases. Because the dependent variable in column 6 is the logarithm of ridership, the estimates imply approximately 4 percent higher ridership during peak hours, 6 percent higher ridership during off-peak hours, and 6 percent higher ridership during weekends. The peak-hour estimate is statistically significant at the 10 percent level, while the off-peak and weekend estimates are statistically significant at the 1 percent level. Evaluated at the mean level of ridership, these effects correspond to approximately 35 additional passengers per route-day during peak hours, 60 additional passengers during off-peak hours, and 84 additional passengers during weekends. The concentration of stronger and more precisely estimated ridership effects outside peak hours is consistent with demand being more

elastic when trips are less constrained by commuting needs and when crowding constraints are less binding.

4.4 Discussion and interpretation

As emphasized in Section 3.2, the estimates in Table 1 are package effects: they capture electrification as it was implemented in Santiago, bundled with fleet renewal, changes in vehicle characteristics, and deployment decisions by operators. The pattern of results disciplines the interpretation. Speed is unchanged, and passenger capacity falls in the periods where ridership rises, so the passenger response runs through neither faster trips nor expanded capacity. The remaining candidates are newer, quieter, and more comfortable vehicles, different deployment across routes and periods, and the reorganization of service that accompanies contract renewal; the data do not separate these channels.

The bundled treatment limits statements about mechanisms, not external validity. Electrification in other cities also arrives through fleet renewal, new procurement contracts, and changes in operations, so the bundle is the policy-relevant object. The substantive lesson is the contrast with bus-priority infrastructure, where ridership gains are mediated by faster travel times (González and Silva, 2025): electric buses move passenger demand through margins other than speed. These demand-side responses, together with the operational responses documented here, enter the welfare accounting in Section 7.

5 Externalities

We now turn to the external effects of electrification, the third term of Eq. (2). This section estimates replacement effects for the three local externalities of bus operations: air pollution, traffic safety, and ambient noise. These are changes in outcomes at fixed locations when electric bus-kilometers replace conventional ones nearby, holding total bus activity fixed. Table 2 collects the headline estimates and expresses each as the effect of moving nearby bus service from fully conventional to fully electric; the full sets of estimates, including additional pollutants, outcomes, exposure radii, and time periods, are reported in Appendix Tables A.1, A.2, and A.3. The evidence is strongest for air pollution, robust for traffic accidents, and suggestive for noise, and we present it in that order.

5.1 Air pollution

The main analysis uses the official air-quality monitoring network, which measures several pollutants at high frequency but at a small number of fixed locations. We complement it with satellite-based $PM_{2.5}$, which offers broad spatial coverage at a coarser monthly frequency and with more spatial smoothing. Both designs estimate the replacement effect defined in Section 3.2: they compare places before and after nearby bus service becomes more electric, relative to other places observed at the same time, holding total bus service fixed.

Data and specification. The monitoring-station analysis combines daily pollution records with the route-level bus operations data. We aggregate validated hourly readings to station-day means for the five pollutants with adequate coverage: $PM_{2.5}$, PM_{10}, CO, NO_2, and NO_x. The PM outcomes are observed at eight stations and the gaseous pollutants at six. The sample runs from January 1, 2022 through April 30, 2025, the period over which bus-kilometers can be reliably linked to the route shapefile.[7]

Exposure follows Section 3.3: for each station we compute total and electric bus-kilometers within circular buffers of 1, 2, 5, and 10 kilometers, with 5 km as the baseline, allocating route-day kilometers in proportion to the route length inside the buffer. Figure A.1 plots the identifying variation: the timing and intensity of electrification differ substantially across stations. The baseline regression for pollutant p at station i on date t is

$$y_{ipt} = \beta_p ElectricKM_{it} + \gamma_p TotalKM_{it} + \alpha_{ip} + \delta_{tp} + \varepsilon_{ipt}, \tag{5}$$

where the treatment variables are measured in units of 10,000 km and α_{ip} and δ_{tp} are station and date fixed effects; the date effects absorb meteorology, seasonality, and citywide pollution episodes. Since $TotalKM_{it}$ is included directly, β_p is the replacement effect. Standard errors are clustered by station; because there are only six to eight clusters, we also report wild cluster bootstrap p-values (Cameron et al., 2008; Webb, 2023).[8]

The satellite check estimates the same specification at the grid-cell-by-month level, using monthly $PM_{2.5}$ from the Van Donkelaar satellite product for 2022–2024 (Shen et al., 2024;

[7]Because route identifiers differ across the operations data and the route shapefile, we use the service dictionary crosswalk to map the route-day identifier to the route-direction identifier in the shapefile. This procedure matches 95.96 percent of citywide bus-kilometers over 2022–2025; the match rate deteriorates sharply after April 2025.

[8]The wild cluster bootstrap p-values for the coefficient on electric bus-kilometers in Table A.1 are 0.069 for $PM_{2.5}$, 0.163 for PM_{10}, 0.011 for NO_x, 0.677 for NO_2, and 0.293 for CO.

Atmospheric Composition Analysis Group, 2025). The panel contains 6,225 cells, of which 804 are ever crossed by the bus network; mean $PM_{2.5}$ among exposed cells is 25.1 $\mu g/m^3$ (Appendix Table A.4). Route-month bus-kilometers are allocated to cells in proportion to the route length inside each cell, using year-specific route geometries; Appendix Figure A.2 maps cumulative exposure.[9] Because the outcome is monthly and spatially smoothed, the satellite design is a complementary check rather than the primary evidence.

Results. Panel A of Table 2 reports the estimates for the three pollutants most closely tied to diesel combustion; Appendix Table A.1 reports all five pollutants and the satellite estimate. The station-level coefficients are negative for all five pollutants. An additional 10,000 electric bus-kilometers within 5 km of a station reduces daily $PM_{2.5}$ by 0.67 $\mu g/m^3$, PM_{10} by 1.08 $\mu g/m^3$, and NO_x by 3.31 ppb. The NO_2 and CO estimates are smaller and imprecise. The evidence is strongest exactly where diesel combustion predicts it: $PM_{2.5}$ and NO_x. The estimates are robust across 1, 2, 5, and 10 km buffers (Appendix Table A.5). The satellite coefficient has the same sign but is much smaller, a reduction of 0.011 $\mu g/m^3$ per 10,000 electric bus-kilometers, and imprecise; the coefficient on total bus-kilometers is positive and significant, which reinforces the importance of conditioning on total bus activity when estimating the effect of fleet composition.

Magnitudes. In the 5 km baseline sample, average nearby bus activity is on the order of 100,000 bus-kilometers per day, so full electrification corresponds to roughly ten units of the treatment. The station estimate therefore implies a reduction of about 6.7 $\mu g/m^3$ in daily $PM_{2.5}$ at an average-exposure monitoring location; a 10 percentage-point increase in the electric share implies one tenth of this effect. The same calculation with the satellite estimate implies only 0.04 $\mu g/m^3$ at the average exposed cell-month: monthly averages over grid cells attenuate a localized roadside channel that daily station data detect. We therefore read the monitoring stations as the primary evidence of local pollution effects and the satellite grid as a broader, more conservative check. These magnitudes also discipline what to expect downstream. Mapped through the estimate of Dardati et al. (2024) that 1 $\mu g/m^3$ of daily $PM_{2.5}$ raises respiratory emergency visits by 0.36 percent, full electrification at an average-exposure location corresponds mechanically to about a 2.4 percent reduction in respiratory ER visits, an implication we examine in Section 6.

[9]The allocation matches 97.2 percent of observed route-month bus-kilometers and 98.2 percent of electric bus-kilometers to the $PM_{2.5}$ grid. When a route-year is unavailable in the corresponding shapefile, we assign the nearest available route geometry from another year.

5.2 Traffic safety

Data and specification. We combine geocoded traffic accidents, with the exact location, date, and severity of each incident, with the route-level bus operations data. Each urban accident in the Metropolitan Region is assigned to the nearest bus route in the corresponding yearly network. The baseline keeps matches within 50 meters; we re-estimate everything at 10 and 100 meters. Appendix Figure A.3 maps the matched accidents over the route network. The outcomes are route-day counts of all accidents, accidents involving injuries, severe incidents, and fatalities. We estimate Poisson pseudo-maximum likelihood (PPML) models

$$\mathbb{E}[Y_{rt} \mid X_{rt}] = \exp\left(\beta\, \text{ElectricShare}_{rt} + \alpha_r + \lambda_t + \log(\text{KM}_{rt})\right), \tag{6}$$

where Y_{rt} is the incident count on route r on day t, $\text{ElectricShare}_{rt}$ is the electric share of route-level bus-kilometers, α_r and λ_t are route and day fixed effects, and $\log(\text{KM}_{rt})$ enters as an exposure term, so β is the replacement effect on incident rates per kilometer traveled. Standard errors are clustered by route. We also estimate an event study at the route-month level, defining treatment as the first month in which the electric share of a route's bus-kilometers exceeds 10 percent and omitting the month before adoption.

Results. Panel B of Table 2 reports the baseline estimates; Appendix Table A.2 reports all four outcomes at the three matching radii. The point estimate for total accidents ranges from -0.21 to -0.22 across radii: a fully electrified route has approximately a 20 percent lower accident rate per kilometer than a comparable diesel route. Accidents involving injuries fall by 21–22 percent (coefficients of -0.24 to -0.25), estimated less precisely but equally stable. Expanding the radius from 10 to 100 meters changes the matched sample considerably yet leaves the coefficients essentially unchanged, so the results do not hinge on the spatial assignment of accidents to routes.

For severe accidents and fatalities the point estimates are also negative but imprecise, as expected for rare events. The exception is the fatality estimate under the strictest 10-meter matching, which is negative and statistically significant at the 5 percent level (Appendix Table A.2, Panel A); it does not persist at wider radii, so we do not lean on it, and excluding fatalities from the welfare valuation in Section 7 is conservative given their sign. The event-study estimates in Figure A.4 show no differential pre-trends for accidents and injuries; the coefficients turn negative after adoption and remain below zero, and the severe and fatality panels are noisy but show no increase. Routes with a higher electric share

therefore experience about one-fifth fewer accidents and injuries per kilometer traveled, and the reduction emerges at the time of electrification rather than reflecting a pre-existing trend.

5.3 Noise

Data and specification. We construct a daily panel of ambient noise from the Ministry of the Environment's monitoring network, obtained through a FOIA request: hourly equivalent sound pressure levels in dB(A) for 12 Santiago stations, January 2022 through December 2024. We aggregate hours to the same workday-peak, workday off-peak, and weekend periods used in the usage analysis, converting readings to acoustic energy, averaging with minute-overlap weights, and converting back to dB(A); station-date-period cells with less than 75 percent of expected minutes are treated as missing. Exposure is built as in the pollution analysis but within 50, 100, and 200 meter buffers, because traffic noise, unlike particulate matter, attenuates within a few hundred meters.

The specification is the common design of Eq. (3), estimated separately by period and buffer, with the treatment and control scaled by average nearby total bus-kilometers so that the coefficient reads directly as the change in dB(A) from moving the average amount of nearby service from zero to fully electric operation. We estimate by OLS and cluster standard errors by station. With only 12 stations, we probe stability by adding station-specific linear trends and by leaving out one station at a time.

Results. Panel C of Table 2 reports the peak-hour estimates; Appendix Table A.3 reports all periods and buffers. During workday peak hours, full electrification of average nearby service lowers ambient noise by 1.43 dB(A) within 50 meters, significant at the 1 percent level; the 100 and 200 meter estimates are similar in size (-1.16 and -1.12 dB(A)) but imprecise. The mean peak-hour level is 63.7 dB(A). Off-peak and weekend estimates are close to zero, the pattern expected if the channel is stop-and-go bus operation when service is most intense. The robustness checks temper the evidence (Appendix Table A.6). Adding station-specific trends shrinks the peak-hour estimate to -0.39 dB(A), no longer significant, and the leave-one-station-out estimates match the baseline at the median but turn positive at the maximum: close-buffer exposure is concentrated around a few stations, and they drive the average. We therefore read the noise evidence as suggestive of a localized peak-hour reduction of roughly one dB(A), not as a precise citywide estimate; the station-trend estimate provides the low scenario in the welfare synthesis.

Interpretation. Vehicle-level studies find larger differences than ours, as they should. Electric buses are about 5 dB(A) quieter than diesel buses during acceleration (Borén, 2020), and replacing diesel-hybrid with electric buses on a corridor cuts indoor low-frequency sound during passages by up to 10 dB, gains that A-weighted measures understate (Glebe et al., 2024). Our outcome is ambient A-weighted noise at outdoor monitors, which pools bus passages with every other sound source. A peak-hour reduction of about one dB(A) is the plausible diluted counterpart of those source-level differences, and it likely understates the perceived improvement for residents living directly along bus corridors.

6 Downstream Effects

The externality estimates establish that electrification reduced local air pollution along the network. This section asks whether those reductions reappear downstream, in respiratory emergency visits and school absenteeism. As Section 3.1 makes clear, these outcomes add no separate welfare term: they are implications of the pollution term under a concentration–response mapping, and we use them to discipline magnitudes. The published estimates that anchor this mapping imply effects that are small relative to the variation in these outcomes, so we present the evidence as a validation exercise. The question is whether the downstream data are consistent with the pollution channel, not whether they can independently detect it.

6.1 Emergency respiratory visits

We first ask whether the pollution reductions are reflected in emergency-room visits for respiratory conditions. The records identify the health center where the patient was treated, not the patient's residence, so we assign exposure using bus service around the center. This is a natural approximation if patients visit nearby centers, but it can also capture changes in health-center utilization, catchment areas, or access to care. We therefore read the emergency-room estimates as suggestive evidence on downstream morbidity.

We construct a balanced weekly panel of the 95 public emergency centers located within 2 km of the route network, from January 2022 through April 2025. For each center and week, we aggregate visits for respiratory causes and construct a non-respiratory comparison outcome as total visits minus respiratory visits; Appendix Figure A.5 plots the raw series.

Our preferred specification defines high electric-bus adoption as the first week in which the electric share of bus-kilometers within 2 km of the center reaches 20 percent.[10] We then estimate event-window regressions of the form:

$$Y_{it} = \beta_1 \mathbf{1}0 \leq \tau_{it} \leq 52 + \beta_2 \mathbf{1}\tau_{it} > 52 + \gamma TotalKM_{it} + \alpha_i + \lambda_t + \varepsilon_{it}, \tag{7}$$

where τ_{it} is the number of weeks since health center i first reached high adoption, $TotalKM_{it}$ is total bus-kilometers within 2 km of the center, and α_i and λ_t are health-center and week fixed effects. For count outcomes we estimate the model by PPML; we also estimate specifications for the respiratory share of visits and for the log ratio of respiratory to non-respiratory visits.

Table 3 reports the results. The point estimates for respiratory visits are negative, falling by 1.9 percent during the first year after high adoption and by 6.0 percent thereafter, but imprecise. More importantly, the non-respiratory comparison outcome moves similarly, falling by 1.0 and 6.2 percent, and the respiratory share and the log ratio show little evidence of a differential decline. The signs are consistent with the pollution mechanism, but the pattern is not respiratory-specific. The event-study estimates in Appendix Figure A.6 show no strong differential pre-trends, but the post-adoption coefficients are noisy and reveal no sharp respiratory-specific break.[11]

We therefore do not interpret the emergency-room results as clean causal evidence of downstream health effects. The estimates are consistent with the pollution channel, but visits measured at the treating facility, with no link to residential exposure, cannot distinguish that channel from changes in emergency-center utilization.

6.2 Student absenteeism

We next examine student absenteeism. Children are especially sensitive to air pollution, and school absences provide a broad measure of morbidity that captures responses not severe

[10] The event-window estimates require roughly one year (49 weeks) of pre-treatment observations, so we drop 27 treated centers that crossed the 20 percent threshold too early in the panel. The estimating sample contains 68 centers, and the first crossing among the retained treated centers occurs in the week of December 12, 2022.

[11] Appendix Table A.7 shows that this conclusion is robust to restricting the sample to SAPU centers and to excluding large-volume, low-volume, or unstable centers. Across these samples, respiratory visits tend to decline after high adoption, especially in later weeks, but non-respiratory visits often decline as well.

enough to generate emergency visits. A growing literature finds that pollution increases absences: Currie et al. (2009) show that carbon monoxide raises school absences in Texas, and Chung et al. (2025) estimate that a 10 μg/m^3 increase in daily $PM_{2.5}$ increases full-day absences by 5.7 percent. These estimates benchmark whether the pollution reductions induced by electrification are large enough to move school attendance.

We construct a monthly school-level panel from MINEDUC administrative attendance records, covering regular primary-school students in grades 1–8 and the months of March through December of each year from 2022 to 2025. The outcome is the school-month absence rate: the number of possible student-days missed divided by the number of possible student-days, so students are weighted by their possible attendance days. The estimation sample uses schools located within 5 km of at least one bus route, a common spatial sample across the alternative exposure buffers.[12] Exposure is built as in the pollution analysis: we allocate route-level daily bus-kilometers to buffers of 500 meters, 1 km, 2 km, and 5 km around each school in proportion to the route length inside each buffer, and aggregate to the school-month level. The specification is the common design of Eq. (3) at the school-month level: we regress the absence rate on electric bus-kilometers within a buffer, controlling for total bus-kilometers within the same buffer, with school and month-year fixed effects. Standard errors are clustered by school.

Table 4 reports the results. Across all four buffers, the coefficients on electric bus-kilometers are small and statistically indistinguishable from zero. The point estimates are negative at 500 meters, 1 km, and 2 km and positive at 5 km, but none is precise, and translating them into the effect of full electrification of the average amount of nearby bus service yields magnitudes close to zero.

These nulls are what the pollution estimates imply. Using the estimate in Chung et al. (2025), a 1 μg/m^3 reduction in $PM_{2.5}$ implies roughly a 0.57 percent reduction in student absences. At the sample mean absence rate of 19.75 percentage points, this corresponds to only about 0.11 percentage points, small relative to the variation in monthly school-level absence rates. Two features of our setting reinforce this interpretation. First, our data are monthly and aggregated at the school level, while the strongest evidence in the literature comes from daily pollution shocks and daily attendance, so aggregation dilutes short-lived responses. Second, buses are only one component of exposure: students face pollution at

[12]School coordinates come from the MINEDUC school directory. Because some schools have missing coordinates in some years but valid coordinates in others, we append the annual directories and use all available years to construct a school-level location, which we then merge to the panel by school and year.

school, at home, and while commuting, so the relevant change in personal exposure is smaller than the local reduction we measure near routes.

Overall, the absenteeism results show no measurable response, and they should not be read as evidence against the pollution channel documented in Section 5.1: given the size of the estimated $PM_{2.5}$ reductions and the effect sizes in the literature, the downstream effect on school-month absenteeism is expected to be small and difficult to detect.

7 Welfare Synthesis

Section 2.3 established that the re-tenders electrified the fleet at approximately no additional resource cost, so the welfare effect of electrification in Eq. (2) reduces, to first order, to the transit-market and external effects estimated in Sections 4 through 6. This section prices those responses. We proceed in two steps that mirror the structure of the estimates: benefits per 10,000 electric bus-kilometers, the unit in which Table 2 reports the replacement effects, and the implied citywide annual flow for the rollout realized between 2022 and 2025.

Three conventions apply throughout. All values are expressed in US dollars of December 2025, converted at the exchange rate of December 31, 2025, and discounted, where a time dimension arises, at the official social discount rate of 5.5 percent.[13] Wherever an official Chilean social price exists we use it, drawing on the published literature only for dose–response relationships that have no official counterpart. Because the valuation of avoided mortality dominates the total and the two defensible conventions differ by a factor of about four, we report every mortality-driven figure under both: the full statistical-life value (VVE) and a life-years valuation (VLY). For every other modeling choice we take the conservative branch and show the alternatives in the sensitivity analysis.

7.1 Prices and parameters

Table 5 collects every price, dose–response coefficient, and quantity used in this section, with sources. Three features deserve comment. First, the prices are the official social prices of the Chilean public investment-evaluation system (Ministerio de Desarrollo Social y Familia, 2026): a value of a statistical life of 60,000 UF (USD 2.62 million), a social

[13] USD 1 = CLP 911.18; UF 1 = CLP 39,727.96 = USD 43.60.

price of carbon of USD 78.8 per ton of CO_2, and social prices of electricity, diesel, and new buses. Using the government's own appraisal prices disciplines the exercise: these are the values against which every Chilean public investment is evaluated. Second, for responses without an official price we use the causal estimates already introduced: the acute mortality response of Deryugina et al. (2019), the emergency-room response of Dardati et al. (2024), the absenteeism response of Chung et al. (2025), and a road-noise hedonic depreciation of 0.40 percent of property value per dB(A), the central value of the meta-analysis literature (Nelson, 2008). Third, the quantities that convert per-location estimates into aggregates come from our own data construction: census population and dwelling counts intersected with the route network, residential values from observed transactions, route-matched accident records, and the administrative bus-kilometer and validation panels.

7.2 The benefits of replacement

Each benefit is the product of one causal estimate from Table 2 and one price from Table 5; Panel A of Table 6 collects the resulting citywide annual flows. We state each product once.

Air pollution. The monitoring-station coefficient implies that 10,000 electric bus-kilometers per day within 5 km of a location reduce daily $PM_{2.5}$ by 0.674 $\mu g/m^3$. This roadside estimate cannot be extrapolated to the 6.4 million people living within 5 km of electrified corridors: applied to their population-weighted exposure, it would imply a population-average reduction of up to 7.5 $\mu g/m^3$ in 2025, more than buses can plausibly account for. We therefore cap the population-average reduction at the bus-attributable share of ambient concentrations. Motor vehicles contribute 37 percent of ambient $PM_{2.5}$ in central Santiago (Barraza et al., 2017), and diesel buses emit about a quarter of transport-sector black carbon (Climate and Clean Air Coalition, 2017), placing the bus contribution near 9 percent, about 1.9 $\mu g/m^3$ at an ambient level of 20 $\mu g/m^3$. Full electrification removes at most this amount; the realized reduction in each year is the cap scaled by the electric share of bus-kilometers, 0.24 $\mu g/m^3$ in 2022 rising to 0.77 $\mu g/m^3$ in 2025. Combined with the acute mortality response of Deryugina et al. (2019), applied to the 1.22 million residents aged 60 and older, these reductions avoid about 74 premature deaths per year in 2022 and 237 in 2025.[14]

We value these deaths under two conventions and report both throughout. The first

[14]The response is estimated for ages 65 and over; we apply it to the population aged 60 and older and state the transfer explicitly. The uncapped roadside aggregation and the satellite-based coefficient provide the high and low scenarios for the pollution scaling.

applies the full VVE, the statistical-life value used throughout the Chilean investment-evaluation system. Because the VVE is calibrated on prime-age adults while acute pollution mortality falls disproportionately on the frail elderly, this is an upper bound on the mortality benefit. The second follows the life-years metric that Deryugina et al. (2019) emphasize for acute elderly mortality. Their preferred estimates, 2.99 life-years and 0.69 deaths per million elderly per μg/m^3-day, imply 4.3 life-years lost per death. We price each life-year at USD 163,000, the VVE annuitized at the 5.5 percent social discount rate over a 40-year prime-age horizon, so each avoided death is worth USD 706,000, and the avoided deaths correspond to 320 to 1,030 life-years per year. The resulting mortality row rises from USD 194 million in 2022 to USD 620 million in 2025 at the VVE, and from USD 52 million to USD 167 million at the VLY; under either convention it is the largest benefit line.[15]

Traffic safety. Full electrification reduces accident rates per kilometer by 20 percent and injury rates by 22 percent. The 2022 baseline within 50 meters of electrified routes is 6,715 accidents involving 9,065 people, of which 2,175 caused injuries (2,936 people) and 73 a death (77 people). Applied to this baseline, these reductions imply about 1,340 fewer accidents and 650 fewer injured per year on this network at full electrification. Priced at the official CONASET (2024) social costs under the local composition of accidents and injuries, this is about USD 14.0 million of avoided vehicle-damage cost and USD 1.3 million of avoided injury cost per year, roughly USD 15 million annually for the electrified network.[16] We do not value the fatality point estimates, which are negative but too imprecise; given their sign, this choice is conservative.

Noise. Full electrification of average nearby service lowers peak-hour ambient noise by 1.43 dB(A) within 50 meters of the corridor. At a noise depreciation index of 0.40 percent per dB(A), the implied capitalization is $0.40 \times 1.43 = 0.57$ percent of the value of the residential stock within 50 meters of electrified corridors. That stock is 815,067 dwellings with a mean transaction value of about USD 131,000, or roughly USD 106 billion in total. Capitalized and annualized at 5.5 percent, full electrification of this stock implies a noise benefit of about USD 33 million per year, which the citywide trajectory scales by the realized electric share

[15]The morbidity row applies the 0.36 percent response of Dardati et al. (2024) to the 734,764 baseline respiratory emergency visits recorded in exposed areas in 2022, priced at the FONASA free-choice tariff for an emergency-medicine consultation, USD 19.9 (FONASA, 2024): between 640 and 2,000 avoided visits per year, under USD 40,000. Because the VVE already prices fatality risk, the morbidity row is additive only under a cost-of-illness reading, which we adopt.

[16]The local composition is 77, 7, and 16 percent slight, less-serious, and serious injuries, and 8, 30, 59, and 3 percent run-over, crash, collision, and rollover accidents, giving weighted costs of USD 10,500 per accident and USD 1,960 per injured person.

(Table 6). Using the median rather than the mean transaction value lowers the stock to USD 85 billion and the benefit in proportion. The station-trend estimate of −0.39 dB(A) generates the low scenario, and zero is a defensible floor given the robustness discussion in Section 5.3.

Carbon. Replacing 10,000 diesel bus-kilometers with electric operation saves a net 15 tons of CO_2: about 18.2 tons of avoided diesel combustion against 3.2 tons from the charging electricity at the current grid emission factor.[17] At the Chilean social price of carbon, USD 78.8 per ton, the central case is about USD 1,180 per 10,000 electric bus-kilometers, in a range of USD 770 to 2,860 as the price moves between USD 51 and USD 190 (Interagency Working Group on Social Cost of Greenhouse Gases, 2021; U.S. Environmental Protection Agency, 2023).

Fare revenue. Full electrification raises ridership by approximately 35, 60, and 84 passengers per route-day in the peak, off-peak, and weekend samples. Valued at the 2025 adult bus fare of CLP 770 (USD 0.85) (Directorio de Transporte Público Metropolitano, 2026), this is on the order of USD 30 to 71 per route-day and period. Scaling the period-specific ridership responses by the realized electric share and the annual bus-validation series yields a citywide fare-revenue gain that grows with the rollout, from about USD 2 million in 2022 to USD 9 million in 2025 (Table 6). We use the fare a rider pays, which is a lower bound on willingness to pay, and add no consumer-surplus term, so the transit-market row is a lower bound on rider benefits.

Table 6 converts the per-unit flows into the citywide annual effect of the realized rollout, scaling each replacement effect by that year's electric bus activity and by the exposure aggregates above, and reports the full 2022–2025 trajectory as the electric share of bus service rises from 13 to 42 percent. The 2025 flow is USD 668 million at the VVE and USD 215 million at the VLY; per 10,000 electric bus-kilometers, these flows correspond to about USD 43,000 and USD 14,000. The annual state subsidy that closes the operating deficit of the whole system, buses, Metro, and commuter rail combined, was CLP 1,156 billion in 2025, about USD 1.27 billion (Directorio de Transporte Público Metropolitano, 2026). The realized gains from the rollout therefore equal about half of the annual subsidy at the VVE and one-sixth at the VLY.

[17] Diesel: $10{,}000/1.47 \approx 6{,}800$ liters at the homologated fuel economy of 1.47 km per liter (International Council on Clean Transportation, 2022), at 2.68 kg of CO_2 per liter. Electricity: $10{,}000 \times 1.34 = 13{,}400$ kWh at 0.2384 t CO_2e/MWh, the 2023 year-end factor of the Coordinador Eléctrico Nacional.

7.3 The cost side

The structure of the tenders, described in Section 2.3, implies that these benefits were obtained at approximately no additional resource cost, and the official prices themselves make the point compactly. The capital premium of an electric over a diesel urban bus is USD 118,000 at social prices (247,000 against 129,000). Its energy cost per kilometer is USD 0.176 against USD 0.601 for diesel, a 71 percent energy-cost saving, and the transport authority reports operating-cost savings of 66 percent and maintenance savings of 44 percent for electric operation (Directorio de Transporte Público Metropolitano, 2026). A bus in the system runs about 60,000 kilometers per year, and the fleet-provision contracts run for 14 years, matching the useful life the tender framework assigns to an electric bus.[18]

At these values the energy saving alone, USD 0.425 per kilometer, amounts to USD 25,500 per bus-year, with a present value at 5.5 percent of USD 245,000 over the 14-year fleet contract, about twice the capital premium, and USD 145,000 over the 7-year operation contract, still above it. The maintenance saving adds to this margin; the main item on the other side is one battery replacement, since warranties run 5 to 7 years. Consistent with this arithmetic, DTPM reports that the 2023 and 2025 re-tenders reduced annual system payments by CLP 60 and 20 billion (USD 66 and 22 million), respectively. Two consequences follow for how we summarize the evaluation. First, net benefits approximately equal gross benefits, so Table 6 is, to first order, the welfare effect itself. Second, with a net fiscal cost near zero the marginal value of public funds diverges by construction, so we report instead the net social benefit per 10,000 electric bus-kilometers and, as an alternative summary, benefits per dollar of the gross capital premium.

7.4 Cross-validation and sensitivity

An independent benchmark exists for Santiago. Rizzi and De La Maza (2017) estimate marginal external costs for the diesel bus of the pre-electrification fleet, the same Euro III-era technology our design replaces. Expressed in dollars of December 2025 and at the official VVE, their estimates imply a diesel-bus externality of about 87 US cents per driven bus-

[18]System kilometers were 390 to 415 million across an operating fleet of 6,400 to 6,900 buses in 2022–2025 (Directorio de Transporte Público Metropolitano, 2026). Fleet contracts run in 168 monthly quotas; the tender framework assigns electric buses a useful life of 14 years or 1.2 million kilometers (DTPM, 2025), in line with the 14-year bus life documented for United States transit agencies (Avenali et al., 2023). Operation contracts run for 7 years, renewable for up to 7 more.

kilometer in air-pollution health costs, 12.4 cents in accidents, and 5.1 cents in noise.[19] Our per-kilometer savings are of the same order: 9.0 cents in noise and 4.1 cents in accidents excluding fatalities. For pollution, the comparison depends on the mortality convention. At the VLY our valuation is 107 cents, essentially reproducing their figure; at the VVE it is 398 cents, the gap reflecting the annualization of an acute daily mortality response at the full statistical-life value. We read this as agreement, with the spread concentrated exactly where the mortality-valuation convention matters.

The benchmark also clarifies what electrification cannot claim. Congestion and road damage, two of their externality components, are unchanged by fleet replacement: our operating-speed estimates are precise zeros, and electric buses are not lighter. We exclude both from the valuation. Finally, their passenger-kilometer comparison (4 cents for the bus against 41 to 42 cents for the car at peak) quantifies the margin our design does not capture: every rider drawn from a car adds unpriced externality gains, so the totals in Table 6 are conservative on this margin as well. Panel B of Table 6 collects the sensitivity of the 2025 total to the three remaining choices, the carbon price, the noise estimate, and the pollution scaling; the mortality valuation is not a sensitivity but the dual VVE/VLY headline reported throughout.

8 Conclusion

We have used the staggered, contract-driven rollout of electric buses in Santiago to estimate what fleet electrification delivers on the ground. Because each route's electrification timing was fixed by contracts written before electrification entered the policy agenda, we compare the same routes and locations before and after their service becomes more electric, holding total bus service fixed. The picture is consistent. Replacing diesel with electric service lowers local air pollution, cuts traffic accidents by about 20 percent, reduces ambient noise near the busiest corridors, and raises ridership, while leaving operating speeds unchanged. Effects on

[19] Per driven bus-kilometer, in USD of 2015, their estimates are 23.2 cents of $PM_{2.5}$-precursor health costs, 15.3 cents through ozone precursors, 5.5 cents of accidents, and 4.2 cents of noise, with congestion the largest component of a peak-hour total of USD 1.80. We inflate their 2015 pesos to December 2025 by the change in the UF (a factor of 1.55) and rescale their mortality-driven components from their VSL (USD 1.16 million of 2015, the mean of their uniform range) to the official VVE, a ratio of 1.87. Our per-kilometer figures divide the full-electrification benefit in Table 6 by 2025 total bus-kilometers (373.7 million). The two approaches also measure different objects, a composition effect at fixed service against the cost of an additional kilometer, so the comparison is of orders of magnitude.

respiratory emergencies and school absenteeism are too small to detect, as the size of the pollution reductions leads us to expect. Valued at official social prices, these benefits amount to USD 215 to 668 million per year in 2025, depending on the mortality valuation, between one-sixth and one-half of the annual public subsidy to the system. The design of the tenders drove the incremental resource cost of the switch close to zero.

Two features make this more than a local evaluation. First, the adopter is the state. The returns therefore do not hinge on the household adoption and utilization margins that limit green-transition instruments working through private choices, and they accrue directly to the people who live, walk, and wait along bus corridors. Second, against the menu of second-best transport policies, electrification is unusual: it buys gains on several margins at once without the offsetting cost that most instruments carry on another. For the growing number of cities committed to zero-emission fleets, two lessons follow. The near-zero cost was engineered rather than automatic, since the tenders spread the capital premium of the electric fleet against its lower energy and maintenance costs. And because our design cannot identify where new riders come from, any diversion from private cars would add unpriced external gains, so the social return is likely larger than we estimate.

Several features bound what these estimates establish. They are package effects, capturing electrification as governments implement it, bundled with fleet renewal and new operations. They are also local and relative: displaced diesel buses may run elsewhere until they retire, so the estimates reflect the reallocation of bus emissions across space, and citywide general-equilibrium effects are absorbed by our time controls. Two channels travel less well than the headline. The carbon savings scale with the emissions intensity of the grid, which in Chile is decarbonizing quickly, so the same fleet would deliver different carbon gains elsewhere. And the Euro III diesel baseline replaced is dirtier than the incumbent fleets of many high-income cities, which raises the pollution and health returns relative to those settings. The outcomes we measure least well, downstream health and ambient noise, are also those where our data are coarsest, so we read that evidence as suggestive.

As cities decarbonize urban travel, public transport is a margin where the state controls adoption directly and where the new technology replaces some of the dirtiest vehicles on the road. Santiago shows that the realized returns to pulling this lever can be large, and that with the right contract design they can be obtained at little additional public cost.

References

Acemoglu, D., U. Akcigit, D. Hanley, and W. R. Kerr (2016, February). Transition to clean technology. *Journal of Political Economy 124*(1), 52–104.

Acemoglu, D., J. Moscona, and J. A. Robinson (2016). State capacity and american technology: Evidence from the nineteenth century. *American Economic Review: Papers & Proceedings 106*(5), 61–67.

Arkolakis, C., K. T. Gillingham, and S.-Y. Yoo (2025). Optimizing electric vehicle infrastructure. *AEA Papers and Proceedings 115*, 563–567.

Assunção, J., C. Gandour, and R. Rocha (2023). DETER-ing deforestation in the Amazon: Environmental monitoring and law enforcement. *American Economic Journal: Applied Economics 15*(2), 125–156.

Atmospheric Composition Analysis Group (2025). Monthly global estimates of fine particulate matter, V6.GL.03. Washington University in St. Louis. Satellite-derived $PM_{2.5}$ product, South America monthly files.

Avenali, A., G. Catalano, M. Giagnorio, and G. Matteucci (2023). Assessing cost-effectiveness of alternative bus technologies: Evidence from US transit agencies. *Transportation Research Part D: Transport and Environment 117*, 103648.

Avenali, A., G. Catalano, M. Giagnorio, and G. Matteucci (2024). Factors influencing the adoption of zero-emission buses: A review-based framework. *Renewable and Sustainable Energy Reviews 197*, 114388.

Banerjee, A., E. Duflo, C. Imbert, S. Mathew, and R. Pande (2020). E-governance, accountability, and leakage in public programs: Experimental evidence from a financial management reform in india. *American Economic Journal: Applied Economics 12*(4), 39–72.

Barahona, N., F. A. Gallego, and J.-P. Montero (2020). Vintage-specific driving restrictions. *Review of Economic Studies 87*(4), 1646–1682.

Barraza, F., F. Lambert, H. Jorquera, A. M. Villalobos, and L. Gallardo (2017). Temporal evolution of main ambient $PM_{2.5}$ sources in Santiago, Chile, from 1998 to 2012. *Atmospheric Chemistry and Physics 17*(16), 10093–10107.

Barwick, P. J., S. Li, A. Waxman, J. Wu, and T. Xia (2024). Efficiency and equity impacts of urban transportation policies with equilibrium sorting. *American Economic Review 114*(10), 3161–3205.

Basso, L. J. and H. E. Silva (2014). Efficiency and substitutability of transit subsidies and other urban transport policies. *American Economic Journal: Economic Policy 6*(4), 1–33.

Bento, A., D. Kaffine, K. Roth, and M. Zaragoza-Watkins (2014). The effects of regulation in the presence of multiple unpriced externalities: Evidence from the transportation sector. *American Economic Journal: Economic Policy 6*(3), 1–29.

Bollinger, B., K. T. Gillingham, and A. J. Kirkpatrick (2025). Valuing solar subsidies. Working Paper 33368, National Bureau of Economic Research.

Borén, S. (2020). Electric buses' sustainability effects, noise, energy use, and costs. *International Journal of Sustainable Transportation 14*(12), 956–971.

Borenstein, S. and J. B. Bushnell (2022). Headwinds and tailwinds: Implications of inefficient retail energy pricing for energy substitution. *Environmental and Energy Policy and the Economy 3*, 37–70.

Cameron, A. C., J. B. Gelbach, and D. L. Miller (2008). Bootstrap-based improvements for inference with clustered errors. *Review of Economics and Statistics 90*(3), 414–427.

Chicago Transit Authority (2022). Charging forward: CTA bus electrification planning report. Technical report, Chicago Transit Authority, Chicago.

Chung, S., C. Persico, and J. Liu (2025). The effects of daily air pollution on students and teachers. Working Paper 33549, National Bureau of Economic Research.

Climate and Clean Air Coalition (2017). Santiago adopts Euro VI buses: A case study. Technical report, Climate and Clean Air Coalition.

CONASET (2024). Costo social de los siniestros de tránsito en Chile 2024. Technical report, Comisión Nacional de Seguridad de Tránsito, Observatorio de Datos, Ministerio de Transportes y Telecomunicaciones, Santiago, Chile. `https://www.conaset.cl/wp-content/uploads/2025/12/Costos-Siniestros-2024.pdf`.

Currie, J., E. A. Hanushek, E. M. Kahn, M. Neidell, and S. G. Rivkin (2009). Does pollution increase school absences? *Review of Economics and Statistics 91*(4), 682–694.

Currie, J. and R. Walker (2011). Traffic congestion and infant health: Evidence from E-ZPass. *American Economic Journal: Applied Economics 3*(1), 65–90.

Dardati, E., R. de Elejalde, and E. Giolito (2024). On the short-term impact of pollution: The effect of PM 2.5 on emergency room visits. *Health Economics 33*(3), 482–508.

Davis, L. W. (2024). The economic determinants of heat pump adoption. *Environmental and Energy Policy and the Economy 5*, 162–199.

Davis, L. W. (2025). What matters for electrification? Evidence from 70 years of U.S. home heating choices. *Review of Economics and Statistics 107*(3), 668–684.

Deryugina, T., G. Heutel, N. H. Miller, D. Molitor, and J. Reif (2019). The mortality and medical costs of air pollution: Evidence from changes in wind direction. *American Economic Review 109*(12), 4178–4219.

Dhaliwal, I. and R. Hanna (2017). The devil is in the details: The successes and limitations of bureaucratic reform in india. *Journal of Development Economics 124*, 1–21.

Directorio de Transporte Público Metropolitano (2026). Informe de gestión 2025. Technical report, DTPM, Gobierno de Chile.

DTPM (2025). Informe de electromovilidad 2025. Technical report, Directorio de Transporte Público Metropolitano, Gobierno de Chile.

European Alternative Fuels Observatory (2022). Alternative fuels observatory. `https://alternative-fuels-observatory.ec.europa.eu/`. Accessed June 26, 2023.

European Parliament and Council of the EU (2024). Regulation (EU) 2024/1610 amending Regulation (EU) 2019/1242 as regards strengthening the CO_2 emission performance standards for new heavy-duty vehicles. Official Journal of the European Union, L, 2024/1610.

Feger, F., N. Pavanini, and D. Radulescu (2022). Welfare and redistribution in residential electricity markets with solar power. *The Review of Economic Studies 89*(6), 3267–3302.

FONASA (2024). Arancel de prestaciones de salud 2024: Libro Arancel Modalidad Libre Elección. Technical report, Fondo Nacional de Salud, Ministerio de Salud, Santiago, Chile. Código 01 01 330, consulta médica de especialidad en medicina de urgencia: total CLP 18,130 (bonificación FONASA CLP 7,250).

Fun Sang Cepeda, M., K. Gore, and X. Mao (2025). Latin america e-bus market monitor, 2024. Technical report, International Council on Clean Transportation.

Giagnorio, M., M. Börjesson, and T. D'Alfonso (2024). Introducing electric buses in urban areas: Effects on welfare, pricing, frequency, and public subsidies. *Transportation Research Part A: Policy and Practice 185*, 104103.

Gillingham, K. T., M. Ovaere, and S. M. Weber (2025). Carbon policy and the emissions implications of electric vehicles. *Journal of the Association of Environmental and Resource Economists 12*(2), 313–352.

Glebe, D., J. Parra, and K. Persson Waye (2024). Replacing diesel buses with electric buses reduced residential low frequency noise. *Transportation Research Part D: Transport and Environment 137*, 104516.

Gómez-Lobo, A. (2025). Revisiting the Transantiago reform: were all the lessons learned? *Research in Transportation Economics 114*, 101676.

González, F. and H. E. Silva (2025). JUE insight: Efficiency of bus priority infrastructure. *Journal of Urban Economics 146*, 103751.

Greenstone, M., G. He, R. Jia, and T. Liu (2022). Can technology solve the principal-agent problem? Evidence from China's war on air pollution. *American Economic Review: Insights 4*(1), 54–70.

Hahn, R. W., N. Hendren, R. D. Metcalfe, and B. Sprung-Keyser (2026). A welfare analysis of policies impacting climate change. *American Economic Review 116*(7), 2368–2421.

Hanna, R., E. Duflo, and M. Greenstone (2016). Up in smoke: The influence of household behavior on the long-run impact of improved cooking stoves. *American Economic Journal: Economic Policy 8*(1), 80–114.

Interagency Working Group on Social Cost of Greenhouse Gases (2021). Technical support document: Social cost of carbon, methane, and nitrous oxide. interim estimates under executive order 13990. Technical report, United States Government.

International Council on Clean Transportation (2022, July). Costo total de propiedad de buses eléctricos en santiago de chile. Technical report, ICCT. Fuel economy from MTT/3CV homologation, Res. Ex. N°2243, Transantiago driving cycle.

International Council on Clean Transportation (2024). Simulación de la operación de un bus eléctrico en una ruta de santiago de chile. Technical report, ICCT. TODO: verify exact title.

IQAir (2025). 2024 world air quality report. Technical report, IQAir. Annual $PM_{2.5}$ city averages for 2024.

Jaeger, J. (2025). These countries are electrifying their bus fleets the fastest. World Resources Institute Insights, June 25, 2025. `https://www.wri.org/insights/countries-electrifying-bus-fleets-fastest`.

Karagulian, F., C. A. Belis, C. F. C. Dora, A. M. Prüss-Ustün, S. Bonjour, H. Adair-Rohani, and M. Amann (2015). Contributions to cities' ambient particulate matter (PM): A systematic review of local source contributions at global level. *Atmospheric Environment 120*, 475–483.

King County Metro Transit (2022). Moving to a zero-emission bus fleet: Transition plan. Technical report, King County Metro Transit Department, Seattle.

Lewis-Faupel, S., Y. Neggers, B. A. Olken, and R. Pande (2016). Can electronic procurement improve infrastructure provision? Evidence from public works in India and Indonesia. *American Economic Journal: Economic Policy 8*(3), 258–283.

Metropolitan Transportation Authority (2024). MTA zero-emission transition plan. Technical report, Metropolitan Transportation Authority, New York.

Miller, J., R. Minjares, T. Dallmann, and L. Jin (2017). Financing the transition to soot-free urban bus fleets in 20 megacities. Technical report, International Council on Clean Transportation.

Ministerio de Desarrollo Social y Familia (2026). Precios sociales 2026. Technical report, División de Evaluación Social de Inversiones, Sistema Nacional de Inversiones, Gobierno de Chile.

MMA (2017). Plan de prevención y descontaminación atmosférica para la región metropolitana de santiago (D.S. n°31/2016). Technical report, Ministerio del Medio Ambiente, Gobierno de Chile. Emissions inventory for the year 2015.

Município de São Paulo (2018). Lei nº 16.802, de 18 de janeiro de 2018. Catálogo de Legislação Municipal. http://legislacao.prefeitura.sp.gov.br/leis/lei-16802-de-18-de-janeiro-de-2018.

Muñoz, J. C., M. Batarce, and D. Hidalgo (2014). Transantiago, five years after its launch. *Research in Transportation Economics 48*, 184–193.

Muralidharan, K., P. Niehaus, and S. Sukhtankar (2016). Building state capacity: Evidence from biometric smartcards in india. *American Economic Review 106*(10), 2895–2929.

Muralidharan, K., P. Niehaus, and S. Sukhtankar (2025). Identity verification standards in welfare programs: Experimental evidence from india. *Review of Economics and Statistics 107*(2), 372–392. TODO: add DOI.

Nelson, J. P. (2008). Hedonic property value studies of transportation noise: Aircraft and road traffic. In A. Baranzini, J. Ramirez, C. Schaerer, and P. Thalmann (Eds.), *Hedonic Methods in Housing Markets*, pp. 57–82. New York: Springer.

Okunogbe, O. and V. Pouliquen (2022). Technology, taxation, and corruption: Evidence from the introduction of electronic tax filing. *American Economic Journal: Economic Policy 14*(1), 341–372.

Parry, I. W. and K. A. Small (2009). Should urban transit subsidies be reduced? *The American Economic Review 99*(3), 700–724.

Parry, I. W. H., M. Walls, and W. Harrington (2007). Automobile externalities and policies. *Journal of Economic Literature 45*(2), 373–399.

Rizzi, L. I. and C. De La Maza (2017). The external costs of private versus public road transport in the metropolitan area of santiago, chile. *Transportation Research Part A: Policy and Practice 98*, 123–140.

Scauzillo, S. (2025). Environmental, labor groups say LA Metro's conversion to electric buses is too slow. Los Angeles Daily News, September 24, 2025. Reports LA Metro figures: 95 battery-electric buses, 4.5% of an approximately 2,050-bus fleet.

Schlenker, W. and W. R. Walker (2016). Airports, air pollution, and contemporaneous health. *Review of Economic Studies 83*(2), 768–809.

Shen, S., C. Li, A. van Donkelaar, N. Jacobs, C. Wang, and R. V. Martin (2024). Enhancing global estimation of fine particulate matter concentrations by including geophysical a priori information in deep learning. *ACS ES&T Air 1*(5), 332–345.

The Jakarta Post (2020). Transjakarta wants 10,000 electric buses in service by 2030. The Jakarta Post, December 29, 2. https://www.thejakartapost.com/news/2020/12/29/transjakarta-wants-10000-electric-buses-in-service-by-2030.html.

Transport for London (2023). London reaches major milestone with more than 1,000 zero emission buses. Press release, Transport for London. August 2023. https://tfl.gov.uk/info-for/media/press-releases/2023/august/london-reaches-major-milestone-with-more-than-1-000-zero-emission-buses.

U.S. Environmental Protection Agency (2023). Report on the social cost of greenhouse gases: Estimates incorporating recent scientific advances. Technical report, EPA.

Waxman, A. R., R. Song, R. Kochhar, and A. Bento (2024). Maintaining vehicle emission reduction rates requires policies to remove cars from the road. Working Paper 4954574, SSRN.

Webb, M. D. (2023). Reworking wild bootstrap-based inference for clustered errors. *Canadian Journal of Economics 56*(3), 839–858.

Figure 1: Santiago in comparative perspective

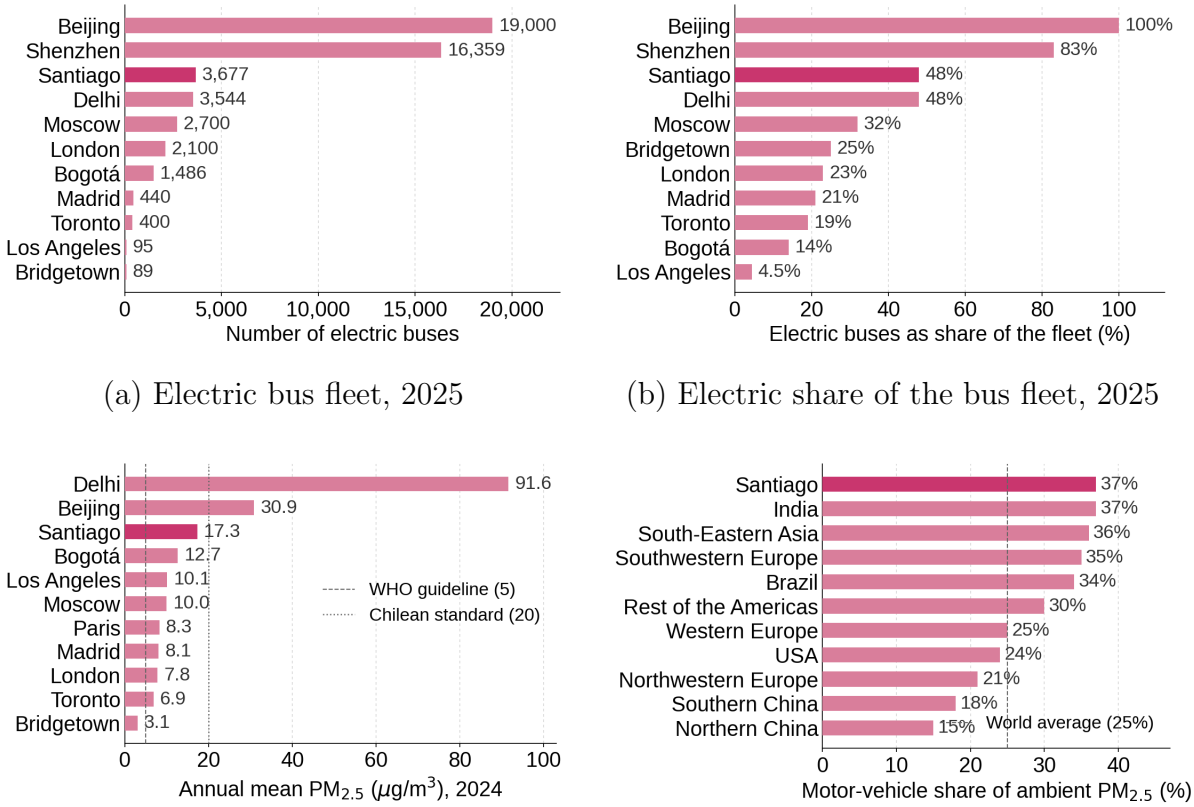

(a) Electric bus fleet, 2025

(b) Electric share of the bus fleet, 2025

(c) Air pollution levels, 2024

(d) Motor-vehicle share of ambient $PM_{2.5}$

Notes. Panels (a) and (b): electric buses in operation and electric buses as a share of the city bus fleet in 2025, from DTPM's Informe de Electromovilidad (DTPM, 2025), based on data from the Centro de Movilidad Sostenible; the Los Angeles figures are those reported by LA Metro as of September 2025 (Scauzillo, 2025). In panel (b), the Informe's chart transposes the Beijing and Shenzhen labels; we report the corrected assignment, consistent with the underlying Centro de Movilidad Sostenible data (Shenzhen's fleet has been fully electric since 2017). Panel (c): annual mean $PM_{2.5}$ concentrations in 2024 (IQAir, 2025); the dashed and dotted lines mark the WHO annual guideline (5 $\mu g/m^3$) and the Chilean annual standard (20 $\mu g/m^3$). Panel (d): motor-vehicle (traffic) share of ambient $PM_{2.5}$; the Santiago estimate comes from 15 years of filter samples in central Santiago (Barraza et al., 2017), and the remaining bars are population-weighted regional averages of urban source-apportionment studies (Karagulian et al., 2015), whose traffic category includes exhaust and non-exhaust vehicle emissions; the dashed line marks the world average (25%).

Figure 2: Buses and electrification

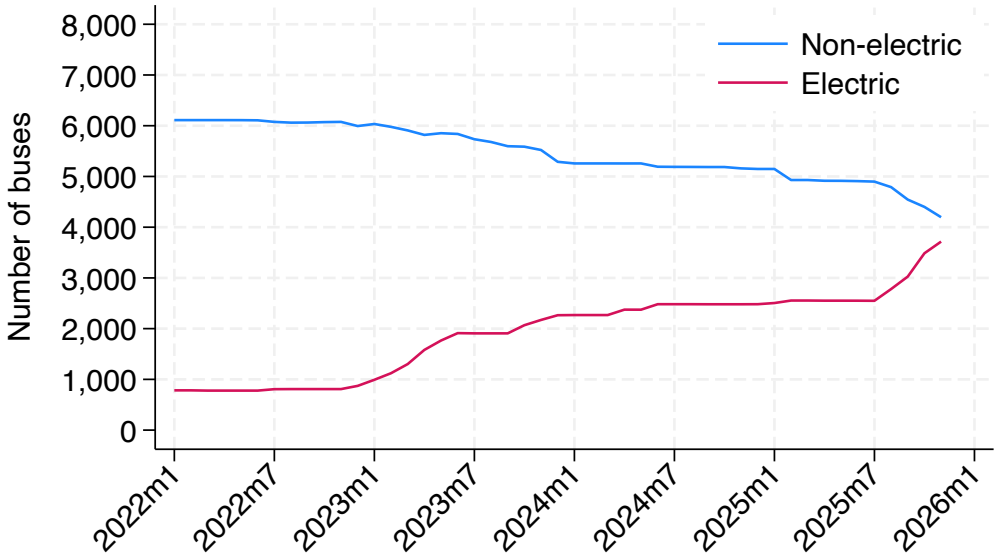

(a) Total number of buses by type

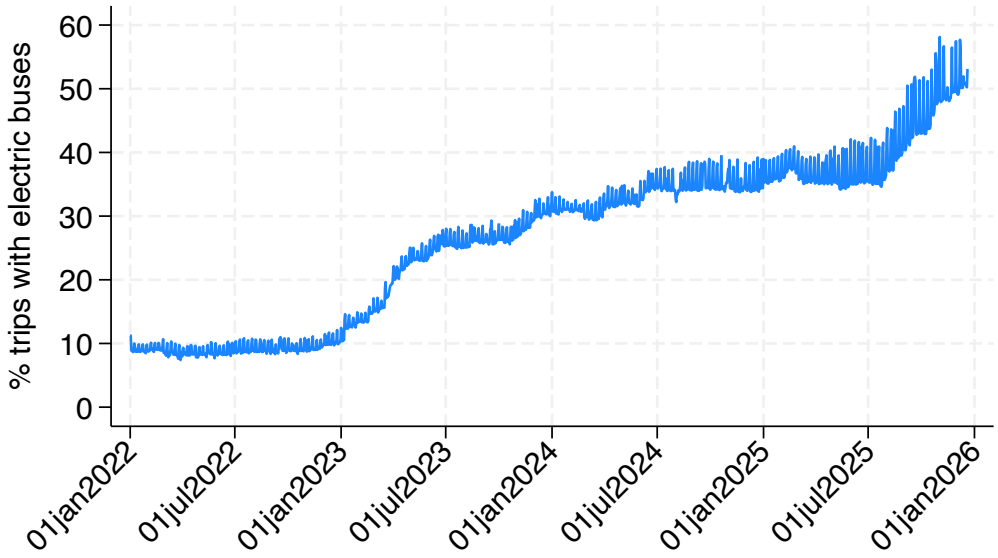

(b) Percentage of trips with electric buses

Notes. The figure documents the electrification of Santiago's bus system over the sample period, from administrative records of the Ministry of Transportation. Panel (a) shows the composition of the operating fleet by propulsion technology, using the bus fleet registry in the first week of each month. Panel (b) shows the share of daily bus trips operated by electric buses, using the trips from all working (non-holiday) Wednesdays of each month.

Figure 3: Bus routes, monitoring stations, health centers, and schools

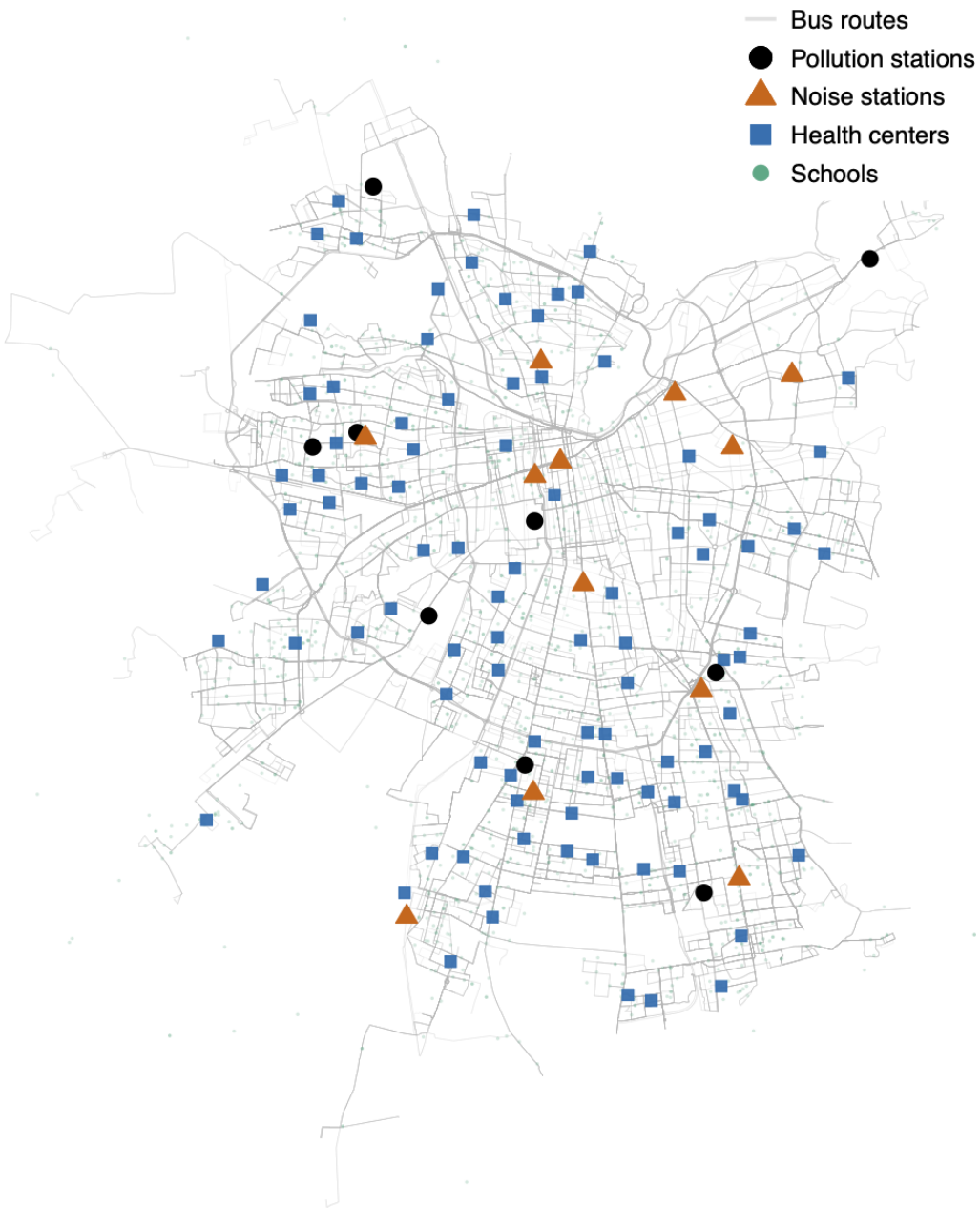

Notes. The figure shows the 2024 bus route network used in the analysis, together with the locations of air-quality monitoring stations, noise monitoring stations, health centers, and schools. Schools are restricted to those located within 5 km of the bus route network.

Table 1: Electric buses, operating speed, and passenger usage

	Service supply				Passenger response	
	Number of buses	Bus-km	Capacity-km	Average speed	Usage	Ridership
	(1)	(2)	(3)	(4)	(5)	(6)
Panel A: Workday peak hours						
Share electric (km)	1.7***	13.9**	-0.32***	-0.09	0.31***	0.04*
	(0.3)	(6.5)	(0.10)	(0.07)	(0.06)	(0.02)
Observations	675,695	675,695	675,695	675,410	675,396	675,396
Routes	1,316	1,316	1,316	1,305	1,316	1,316
Avg. dependent variable	20.9	540	1.44	18.9	1.84	877
Panel B: Workday off-peak hours						
Share electric (km)	4.1***	15.9	0.21	-0.08	0.14***	0.06***
	(0.5)	(9.8)	(0.20)	(0.07)	(0.05)	(0.02)
Observations	620,705	620,705	620,705	620,168	620,705	620,705
Routes	1,299	1,299	1,299	1,293	1,299	1,299
Avg. dependent variable	24.1	755	2.43	20.2	1.50	995
Panel C: Weekend all hours						
Share electric (km)	4.6***	32.8***	-1.25***	-0.00	0.24***	0.06***
	(0.7)	(12.8)	(0.30)	(0.12)	(0.05)	(0.02)
Observations	240,013	240,013	240,013	239,760	240,013	240,013
Routes	1,242	1,242	1,242	1,224	1,242	1,242
Avg. dependent variable	44.75	1,266	7.27	22.9	0.58	1,392

Notes. Daily data at the route level, 1 January 2022 to 31 December 2025; Panel C includes weekends and holidays. Bus-km is the total number of kilometers traveled by buses on a route-day. Capacity-km equals total passenger capacity, including seated and standing capacity, multiplied by kilometers traveled, in millions. Usage is validations divided by available passenger capacity per trip, in percent; ridership, in logarithms, is the total number of paying passengers. All regressions include route and date fixed effects; all except column 2 are weighted by first-60-days bus-km. Robust standard errors, clustered at the route level, are in parentheses. Statistical significance: *** $p < 0.01$, ** $p < 0.05$, * $p < 0.1$.

Table 2: Externality effects of electrification

	Estimate	Full electrification	Observations	Units (clusters)
	(1)	(2)	(3)	(4)
Panel A: Air pollution, per 10,000 electric bus-km within 5 km of stations				
$PM_{2.5}$ ($\mu g/m^3$)	-0.674**	−6.7	9,103	8
	(0.250)			
PM_{10} ($\mu g/m^3$)	-1.076*	−10.8	9,290	8
	(0.521)			
NO_x (ppb)	-3.313*	−33.1	6,854	6
	(1.301)			
Panel B: Traffic safety, electric share of bus-km, incidents within 50 m (PPML)				
Accidents	-0.22*	−20%	548,320	742
	(0.12)			
Injuries	-0.25*	−22%	491,425	657
	(0.14)			
Panel C: Ambient noise in dB(A), workday peak hours				
Within 50 m of station	-1.43***	−1.4	7,903	12
	(0.44)			
Within 100 m of station	-1.16	−1.2	7,903	12
	(0.95)			
Within 200 m of station	-1.12	−1.1	7,903	12
	(1.11)			

Notes. Each panel reports the replacement effect of electrification on one externality; the full sets of estimates are in Appendix Tables A.1, A.2, and A.3. Column (2) expresses each estimate as the effect of moving nearby bus service from fully conventional to fully electric. Panel A: station-day regressions of daily concentrations on electric bus-kilometers (in units of 10,000) within 5 km of the station, controlling for total bus-kilometers, with station and day fixed effects; column (2) evaluates full electrification at the average nearby activity of roughly 100,000 bus-kilometers per day; wild cluster bootstrap p-values are 0.069 ($PM_{2.5}$), 0.163 (PM_{10}), and 0.011 (NO_x). Panel B: route-day PPML estimates with route and day fixed effects and total bus-kilometers as exposure; column (2) reports $(e^{\beta} - 1) \times 100$. Panel C: station-date regressions of peak-hour LAeq on electric bus-kilometers scaled by average nearby total bus-kilometers, controlling for total activity, with station and date fixed effects; the estimate is already in full-electrification units. Standard errors, clustered by station in Panels A and C and by route in Panel B, are in parentheses. Statistical significance: *** $p < 0.01$, ** $p < 0.05$, * $p < 0.1$.

Table 3: Emergency visits after high electric-bus adoption

	Dep. variable: Number of ER visits		Dep. variable: Respiratory composition	
	Respiratory	Non-respiratory	Respiratory share	Log respiratory/ non-respiratory
	(1)	(2)	(3)	(4)
0–52 weeks after high adoption	-0.019	-0.010	-0.002	-0.029
	(0.029)	(0.023)	(0.008)	(0.044)
More than 52 weeks after high adoption	-0.062	-0.064	0.002	-0.036
	(0.055)	(0.048)	(0.015)	(0.082)
Mean dep. variable	234.3	514.9	0.313	-0.847
Health centers	68	68	68	68
Treated centers	57	57	57	57
Never-treated centers	11	11	11	11
Center-week observations	11,764	11,764	11,764	11,764
Health-center fixed effects	Yes	Yes	Yes	Yes
Week fixed effects	Yes	Yes	Yes	Yes

Notes. This table reports estimates from health-center-week regressions of emergency-room visits on indicators for the time elapsed since nearby bus service reached high electric adoption. High adoption is defined as an electric share of at least 20 percent among bus-kilometers within 2 km of the health center. The omitted category is the period before high adoption, including centers that do not reach the threshold during the sample. Columns 1 and 2 are estimated by PPML. Column 3 is estimated by OLS, weighted by total ER visits. Column 4 is estimated by OLS. All regressions include health-center and week fixed effects. Standard errors, clustered by health center, are reported in parentheses.

Table 4: Electric bus adoption and school absenteeism

	Distance to bus routes			
Dependent variable:	Absence rate, percentage points			
Buffer:	500m	1km	2km	5km
	(1)	(2)	(3)	(4)
Electric bus-km, 100k	-0.109	-0.013	-0.011	0.008
	(1.039)	(0.313)	(0.091)	(0.025)
Total bus-km, 100k	-0.073	-0.221	-0.083	-0.032**
	(0.862)	(0.278)	(0.074)	(0.016)
School fixed effects	Yes	Yes	Yes	Yes
Time fixed effects	Month-year	Month-year	Month-year	Month-year
Unit of observation	School-month	School-month	School-month	School-month
Weighted	No	No	No	No
Schools	1,313	1,313	1,313	1,313
Observations	51,995	51,995	51,995	51,995
Avg. dependent variable	19.75	19.75	19.75	19.75

Notes. The table reports school-month estimates of the relationship between electric-bus adoption and absenteeism among primary-school students. The sample includes regular primary-school students in grades 1–8 during March–December of each year from 2022 to 2025. The dependent variable is the school-month absence rate, defined as absent student-days divided by possible student-days and expressed in percentage points. Each column measures bus exposure within the buffer indicated in the column heading. Electric and total bus-kilometers are measured in units of 100,000 km. All specifications control for total bus-kilometers, so the coefficient on electric bus-kilometers captures changes in the composition of nearby bus service holding total bus activity fixed. All regressions include school and month-year fixed effects. Standard errors clustered by school are reported in parentheses. Statistical significance: *** <0.01, ** <0.05, * <0.1.

Table 5: Valuation inputs for the welfare synthesis

Parameter	Value	Source
Prices (USD of December 2025)		
Value of a statistical life (VVE)	USD 2.62 million (60,000 UF)	Ministerio de Desarrollo Social y Familia (2026)
Value per life-year (VLY)	USD 163,000	VVE annuitized, 5.5%, 40 years
VLY value per acute death	USD 706,000 (4.3 life-years)	Deryugina et al. (2019)
Cost per non-fatal injury	USD 1,215 / 1,585 / 5,822	CONASET (2024)
Vehicle-damage cost, bus involved	USD 475 / 9,355 / 14,056 / 18,447	CONASET (2024)
Cost per respiratory ER visit	USD 19.9 (CLP 18,130)	FONASA (2024)
Social price of carbon	USD 78.8/t CO_2 (CLP 71,801)	Ministerio de Desarrollo Social y Familia (2026)
Social cost of carbon, range	USD 51; USD 190	Interagency Working Group on Social Cost of Greenhouse Gases (2021); U.S. Environmental Protection Agency (2023)
Social price of electricity, high tension	USD 0.131/kWh (CLP 119.8)	Ministerio de Desarrollo Social y Familia (2026)
Social price of diesel, bus	USD 0.883/liter (CLP 805)	Ministerio de Desarrollo Social y Familia (2026)
Adult bus fare (2025)	USD 0.85 (CLP 770)	Directorio de Transporte Público Metropolitano (2026)
New urban bus, diesel; electric	USD 129,000; 247,000	Ministerio de Desarrollo Social y Familia (2026)
Annual kilometers per bus	≈60,000	Directorio de Transporte Público Metropolitano (2026)
Fleet contract; electric bus life	14 years; 14 years or 1.2 million km	DTPM (2025)
Noise depreciation index	0.40%/dB(A) [0.16–0.64]	Nelson (2008)
Dose–response		
Acute $PM_{2.5}$ mortality, ages 65+	0.69 deaths/million per $\mu g/m^3$-day	Deryugina et al. (2019)
Acute $PM_{2.5}$ life-years lost, ages 65+	2.99/million per $\mu g/m^3$-day	Deryugina et al. (2019)
Respiratory ER visits	+0.36% per $\mu g/m^3$-day	Dardati et al. (2024)
Full-day school absences	+5.7% per 10 $\mu g/m^3$	Chung et al. (2025)
Quantities		
Electric bus energy use	1.34 kWh/km	International Council on Clean Transportation (2024)
Diesel bus fuel economy	1.47 km/liter [1.39–1.55]	International Council on Clean Transportation (2022)
Grid emission factor (2023, official)	0.2384 t CO_2e/MWh	CEN (2024)
Population within 5 km of corridors	6,380,743 (aged 60+: 1,219,798)	own construction
Dwellings within 50 m; 200 m of corridors	815,067; 2,005,015	own construction
Residential value within 50 m	USD 106 billion (mean sale)	own construction
Baseline respiratory ER visits (2022, 2 km)	734,764	own construction
Baseline accidents/injuries/fatal (2022, 50 m)	6,715 / 2,175 / 73	own construction
Annual electric bus-km, 2022–2025	45.0 / 96.1 / 137.8 / 155.9 million	own construction
Pop.-weighted e-bus-km within 5 km	17.1 / 29.5 / 40.8 / 40.6 million per year	own construction
Bus-attributable share of ambient $PM_{2.5}$	≈9% (≈1.9 $\mu g/m^3$)	Barraza et al. (2017); Climate and Clean Air Coalition (2017)

Notes. All monetary values are US dollars of December 31, 2025, converted at USD 1 = CLP 911.18 and UF 1 = CLP 39,727.96 (USD 43.60). The high-tension electricity price applies to depot charging. The VVE follows the transfer function adopted by the Chilean investment-evaluation system; the noise depreciation index is the central value for road traffic noise, with the bracketed range spanning published meta-analytic estimates. Injury costs are the CONASET (2024) social cost per injured person for slight, less-serious, and serious injuries (27.86, 36.35, and 133.52 UF); fatalities enter through the VVE. Vehicle-damage costs are the CONASET social cost of material damage per vehicle involved, by accident type (run-over, crash, collision, rollover: 10.89, 214.55, 322.37, and 423.10 UF), for a heavy vehicle. The 2023 grid emission factor is the year-end value of the Coordinador Eléctrico Nacional; the 2022, 2024, and 2025 factors are provisional. Baseline accident counts are route-matched within 50 m of electrified routes in 2022. The accident-composition weights and the derivation of the bus-attributable share of ambient $PM_{2.5}$, which caps the population-average effect of full electrification at about 1.9 $\mu g/m^3$, appear in Section 7.2.

Table 6: The welfare effect of electrification

Panel A: citywide annual benefits over the rollout, USD million per year				
	2022	2023	2024	2025
Electric share of bus-km	13.1%	25.0%	34.5%	41.7%
Air pollution: mortality, at VVE	194	372	513	620
at VLY	52	100	139	167
Air pollution: morbidity	0.01	0.02	0.03	0.04
Traffic safety	2.0	3.8	5.3	6.4
Noise	4.4	8.3	11.5	13.9
Carbon	5.3	11.4	16.3	18.5
Fare revenue	2.3	5.2	7.9	9.3
Total, mortality at VVE	208	401	554	668
Total, mortality at VLY	66	129	180	215

Panel B: 2025 total under alternative assumptions, USD million		
	Mortality at VVE	Mortality at VLY
Central case	668	215
Carbon price USD 51 per ton	662	209
Carbon price USD 190 per ton	694	241
No noise effect	654	201
Noise effect of -0.39 dB(A)	658	205
Pollution scaling: satellite-based (low)	81	57
Pollution scaling: uncapped monitor-based (high)	6,030	1,660

Notes. Panel A reports central-case citywide benefits by year, in millions of US dollars of December 2025. Each entry scales a replacement effect from Table 2 by that year's electric bus activity and the exposure aggregates described in Section 7.2. Mortality applies the capped population-average $PM_{2.5}$ reductions (0.24 to 0.77 $\mu g/m^3$, avoiding 74 to 237 deaths per year) to the 1.22 million residents aged 60 and older and values avoided deaths at the VVE (USD 2.62 million) or at the VLY (USD 706,000). Morbidity applies the Dardati et al. (2024) response to baseline respiratory emergency visits at the FONASA tariff. Traffic safety scales the full-electrification benefit (USD 15.4 million) by the electric share of bus-kilometers. Noise applies the -1.43 dB(A) estimate to the residential stock within 50 meters (USD 106 billion), capitalized at 0.40 percent per dB(A) and annualized at 5.5 percent. Carbon values the net saving of 15 t CO_2 per 10,000 electric bus-kilometers at USD 78.8 per ton. Fare revenue applies the period-specific ridership responses, through a blended semi-elasticity of 0.05, to the annual bus-validation series at the CLP 770 (USD 0.85) adult fare. The 2025 totals correspond to CLP 609 and 196 billion. Panel B varies one assumption at a time, holding the rest at central values: the carbon price between USD 51 and 190 per ton, the noise effect between zero and the station-trend estimate of -0.39 dB(A), and the pollution scaling between the satellite-based coefficient (low) and the uncapped roadside aggregation (high), which rescale the mortality row. Panel B entries are recomputations from the Panel A rows, rounded.

ONLINE APPENDIX

Public Transport Electrification: Lessons from a Pioneer

Felipe González and Hugo E. Silva

List of Figures

List of Tables

Figure A.1: Staggered adoption of electric buses around monitoring stations

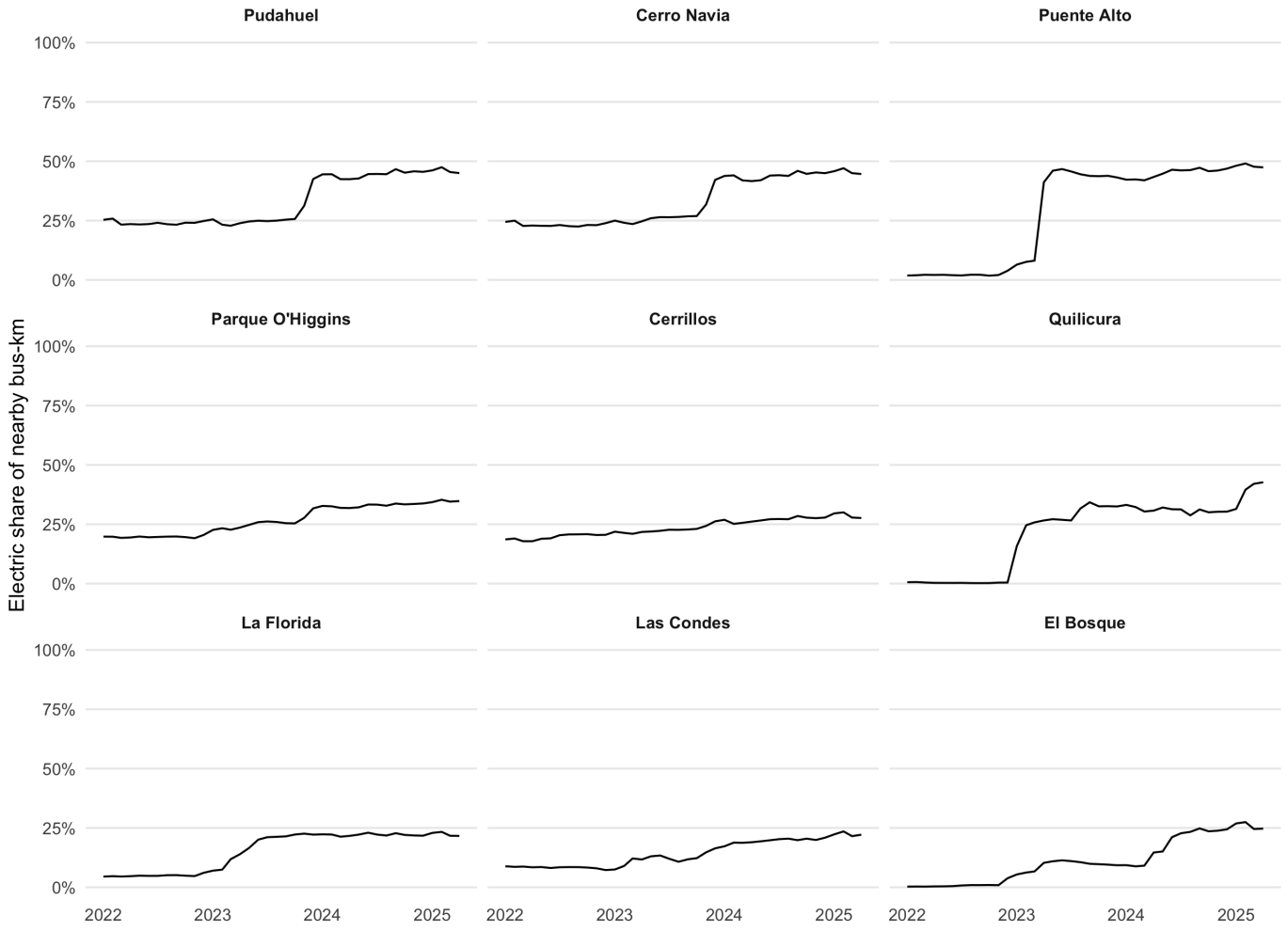

Notes. The figure plots, for each air-quality monitoring station used in the pollution analysis, the monthly average share of bus-kilometers within 5 km of the station operated by electric buses, from January 2022 through April 2025. Route-day bus-kilometers are allocated to station buffers in proportion to the route length inside the buffer. The dispersion in timing and intensity across stations is the identifying variation described in Section 3.3.

Figure A.2: Santiago grid with bus-km

(a) Total bus-km

(b) Electric bus-km

Notes. The figure maps the $PM_{2.5}$ grid used in the analysis and the Santiago bus-route network. Panel (a) shades each grid cell by cumulative allocated bus-kilometers over 2022–2024. Panel (b) shades each grid cell by cumulative allocated electric bus-kilometers over the same period. Bus-kilometers are allocated from route-month observations to grid cells in proportion to the length of each route segment inside the cell. Black lines show route geometries. Legend units are thousands of bus-kilometers.

Figure A.3: Map of traffic safety

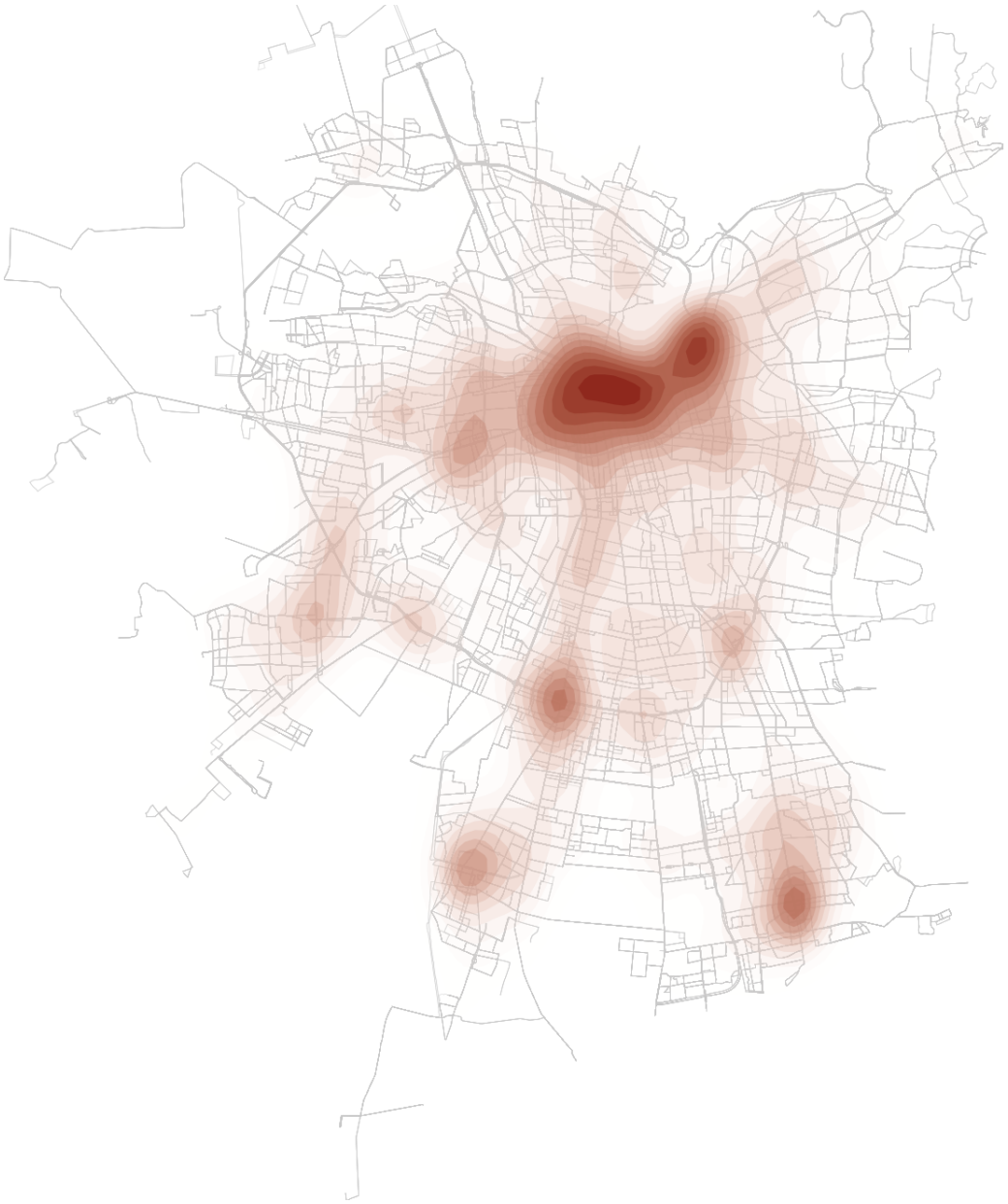

Notes. The figure maps the spatial distribution of traffic accidents matched to the bus-route network in Santiago. Gray lines show bus routes, and red shading shows the density of geocoded accidents assigned to the nearest route within 50 meters, corresponding to the baseline matching radius used in Table A.2. Darker areas indicate higher concentrations of matched accidents. The figure is descriptive and is intended to illustrate the spatial coverage of the accident data and the concentration of incidents across the route network; the regression analysis uses route-day accident counts linked to bus kilometers and electrification.

Figure A.4: Event-study for traffic safety estimates

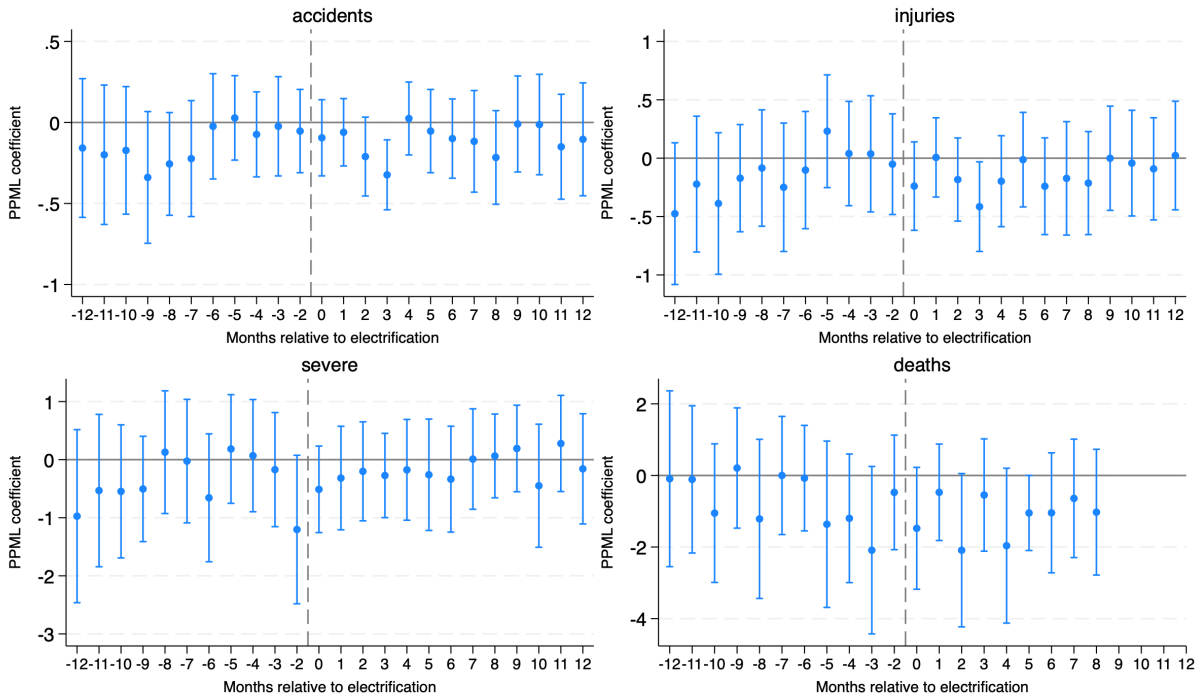

Notes. The figure reports event-study estimates of the relationship between electrification and traffic safety outcomes at the route-month level. The four panels correspond to the number of accidents, injuries, severe incidents, and fatalities, respectively. The coefficients are obtained from Poisson pseudo-maximum likelihood (PPML) regressions with route and calendar-month fixed effects and route-level bus kilometers included as an exposure term. The main explanatory variables are indicators for months relative to the first month in which the share of bus kilometers operated by electric buses exceeds 10% on a route. The month immediately preceding treatment (month -1) is omitted, so all coefficients are interpreted relative to this baseline period. The sample includes routes that are never electrified together with routes that experience electrification during the sample period. Standard errors are clustered at the route level, and the figure displays point estimates with 95% confidence intervals.

Figure A.5: Respiratory ER visits

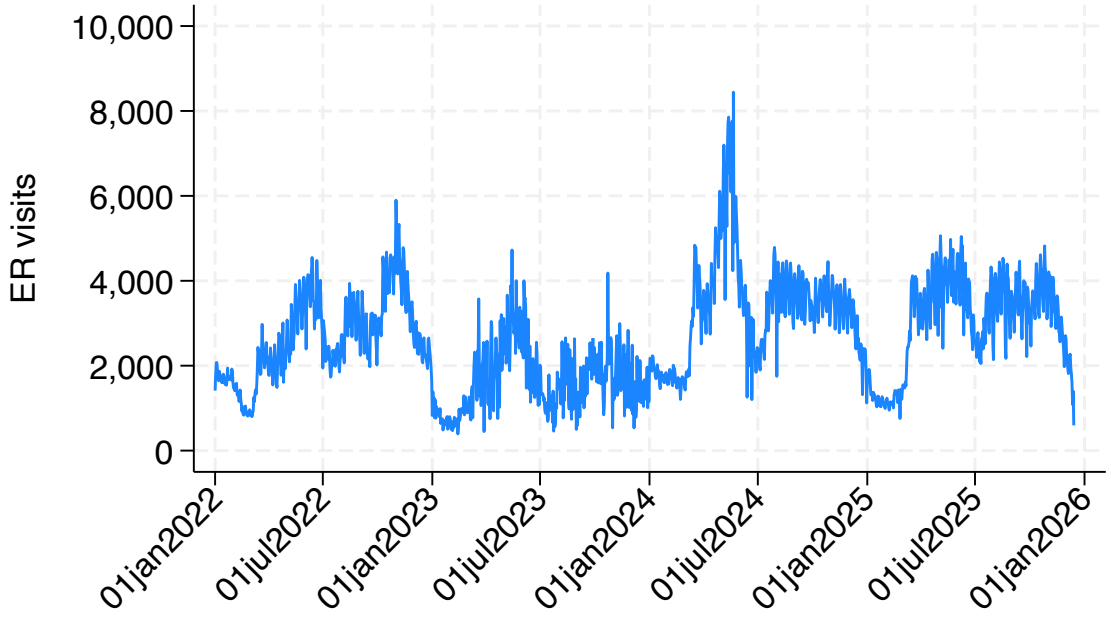

Notes. All ER visits in the 95 health centers located within 2 km of the bus route network. The estimating sample in Table 3 excludes 27 of these centers that reached high electric-bus adoption too early in the panel (see Section 6.1).

Figure A.6: Event study: ER visits around high electric-bus adoption

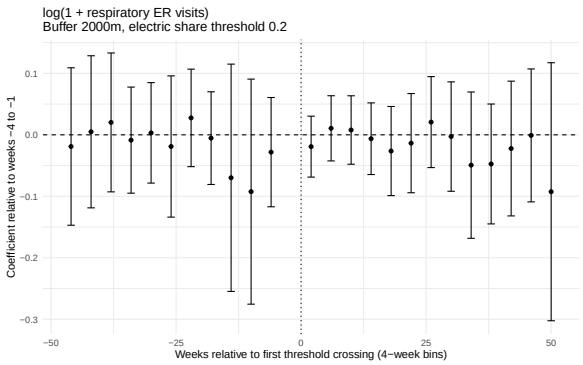

(a) Respiratory ER visits

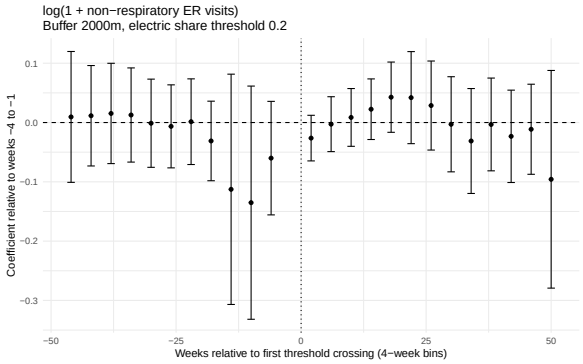

(b) Non-respiratory ER visits

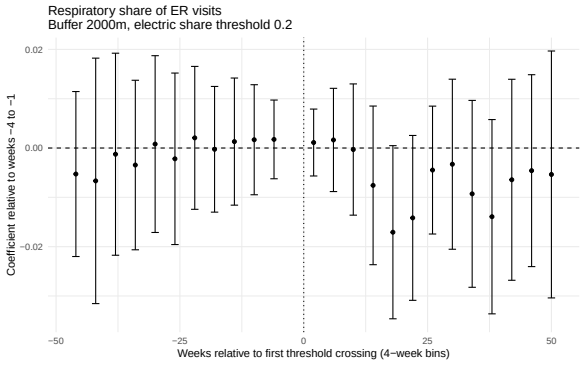

(c) Respiratory share of ER visits

Notes. This figure plots event-study coefficients for emergency-room visits around the first week in which the electric share of bus-kilometers within 2 km of a health center reaches 20 percent. The omitted category is the four-week bin immediately before high adoption. Each coefficient corresponds to a four-week event-time bin. Panels A and B use $\log(1+y)$ outcomes for respiratory and non-respiratory ER visits, respectively. Panel C uses the respiratory share of ER visits. All regressions include health-center and week fixed effects and control for total bus-kilometers within 2 km of the health center. Vertical bars report 95 percent confidence intervals based on standard errors clustered by health center.

Table A.1: Electric bus adoption and pollution

	Monitoring stations					Satellite grid
Dependent variable:	$PM_{2.5}$	PM_{10}	NO_x	NO_2	CO	$PM_{2.5}$
	(1)	(2)	(3)	(4)	(5)	(6)
Electric bus-km, 10k	-0.6737**	-1.076*	-3.313*	-0.1799	-0.0233	-0.0110
	(0.2499)	(0.5208)	(1.301)	(0.4195)	(0.0212)	(0.0240)
Total bus-km, 10k	0.2769*	0.4267	1.999***	-0.0857	0.0126	0.2150***
	(0.1285)	(0.3376)	(0.2738)	(0.2594)	(0.0122)	(0.0320)
Location fixed effects	Station	Station	Station	Station	Station	Grid cell
Time fixed effects	Day	Day	Day	Day	Day	Month-year
Unit of observation	Station-day	Station-day	Station-day	Station-day	Station-day	Cell-month
Observations	9,103	9,290	6,854	6,854	6,767	28,944

Notes. Columns (1)–(5) report monitoring-station estimates using the baseline 5 km exposure buffer. Column (6) reports the satellite-grid estimate using the $PM_{2.5}$ grid-cell panel and the preferred construction with year-specific route geometries when available and the nearest available route geometry otherwise. Electric and total bus-kilometers are measured in units of 10,000 km in all columns. $PM_{2.5}$ and PM_{10} are measured in $\mu g/m^3$ and NO_x in parts per billion (ppb). The original satellite-grid regression is estimated with bus-kilometers measured in thousands; column (6) rescales the coefficient and standard error by a factor of ten. All specifications control for total bus-kilometers, so the coefficient on electric bus-kilometers captures changes in the composition of bus service holding total bus activity fixed. Standard errors are clustered at the station level in columns (1)–(5) and at the grid-cell level in column (6). Statistical significance: *** p <0.01, ** p <0.05, * p <0.1.

Table A.2: Electrification and traffic safety outcomes

Dependent variable: Incident counts (route-level)				
	Accidents	Injuries	Severe	Deaths
	(1)	(2)	(3)	(4)
Panel A: 10-meter radius				
Share electric (km)	-0.22*	-0.24*	-0.31	-1.38**
	(0.12)	(0.14)	(0.22)	(0.63)
Observations	542,833	476,605	264,100	18,176
Routes	732	641	463	141
Mean dep. variable	0.03	0.01	0.01	0.01
Panel B: 50-meter radius (baseline)				
Share electric (km)	-0.22*	-0.25*	-0.26	-0.79
	(0.12)	(0.14)	(0.22)	(0.63)
Observations	548,320	491,425	291,514	22,212
Routes	742	657	488	153
Mean dep. variable	0.03	0.01	0.01	0.01
Panel C: 100-meter radius				
Share electric (km)	-0.21*	-0.24*	-0.23	-0.74
	(0.11)	(0.13)	(0.20)	(0.60)
Observations	552,311	496,562	303,788	24,839
Routes	750	665	500	163
Mean dep. variable	0.04	0.01	0.01	0.01

Notes. The table reports Poisson pseudo-maximum likelihood (PPML) estimates of the relationship between electrification and traffic safety outcomes at the route-day level. Each panel changes the distance threshold used to assign traffic incidents to bus routes: 10 meters in Panel A, 50 meters in Panel B, and 100 meters in Panel C. The dependent variables are counts of accidents, injuries, severe incidents, and fatalities. The main explanatory variable is the share of route-level bus kilometers operated by electric buses. All specifications include route and day fixed effects. Route-level kilometers are included as an exposure term, so coefficients can be interpreted as effects on incident rates per kilometer. Standard errors, clustered at the route level, are reported in parentheses. Coefficients can be interpreted as semi-elasticities: a coefficient β implies a $(e^{\beta} - 1) \times 100$ percent change in the incident rate when the electric share increases from 0 to 1.

Table A.3: Electric bus adoption and noise levels

	Workday peak	Workday off-peak	Weekend/holiday
Panel A: 50m buffer			
Electric bus-km / mean total bus-km	-1.428***	-0.548	-0.249
	(0.437)	(0.556)	(0.352)
Total bus-km / mean total bus-km	0.447**	-0.046	-0.145
	(0.160)	(0.138)	(0.296)
Observations	7,903	7,961	3,715
Stations	12	12	12
Avg. dependent variable	63.73	63.66	61.74
Mean total bus-km nearby	17.8	23.1	36.6
Mean electric share nearby	0.23	0.23	0.25
Panel B: 100m buffer			
Electric bus-km / mean total bus-km	-1.163	-0.132	-0.148
	(0.952)	(0.607)	(0.464)
Total bus-km / mean total bus-km	0.391	-0.115	-0.093
	(0.341)	(0.159)	(0.222)
Observations	7,903	7,961	3,715
Stations	12	12	12
Avg. dependent variable	63.73	63.66	61.74
Mean total bus-km nearby	56.3	74.5	116.5
Mean electric share nearby	0.23	0.23	0.25
Panel C: 200m buffer			
Electric bus-km / mean total bus-km	-1.118	0.174	0.039
	(1.111)	(0.624)	(0.602)
Total bus-km / mean total bus-km	0.384	-0.223	-0.117
	(0.434)	(0.233)	(0.261)
Observations	7,903	7,961	3,715
Stations	12	12	12
Avg. dependent variable	63.73	63.66	61.74
Mean total bus-km nearby	128.7	170.6	265.7
Mean electric share nearby	0.21	0.20	0.23
Station fixed effects	Yes	Yes	Yes
Date fixed effects	Yes	Yes	Yes

Notes. The unit of observation is a noise-monitoring-station by date by time period. The dependent variable is LAeq in dB(A), aggregated from hourly observations by first converting dB(A) values to acoustic energy, averaging energy over the relevant minutes, and converting back to dB(A). The sample covers January 2022 through December 2024, the period covered by the current noise-monitoring files. Electric and total bus-kilometers are measured within the buffer shown in each panel and are divided by the mean total bus-kilometers in the corresponding buffer-period estimation sample. The coefficient on electric bus-kilometers therefore reports the effect, in dB(A), of replacing the average amount of nearby bus activity with electric bus activity, holding total nearby bus activity fixed. All regressions include station and date fixed effects. Standard errors clustered by station are reported in parentheses. Statistical significance: *** $p < 0.01$, ** $p < 0.05$, * $p < 0.1$.

Table A.4: Summary statistics for the $PM_{2.5}$ grid-cell panel

Cells:	All	Ever exposed	Never exposed
	(1)	(2)	(3)
Grid cells	6,225	804	5,421
Cell-months	224,100	28,944	195,156
$PM_{2.5}$ mean	18.37	25.14	17.36
$PM_{2.5}$ standard deviation	7.47	10.39	6.35
$PM_{2.5}$ p10	11.27	15.39	11.04
$PM_{2.5}$ median	16.21	20.67	15.47
$PM_{2.5}$ p90	28.27	41.53	26.59
Total bus-km, mean per cell-month	4,871.7	37,719.3	0.0
Electric bus-km, mean per cell-month	1,221.7	9,459.2	0.0
Non-electric bus-km, mean per cell-month	3,650.0	28,260.1	0.0
Total bus-km, cumulative	1,091,746,539	1,091,746,539	0
Electric bus-km, cumulative	273,787,634	273,787,634	0
Electric share of bus-km	25.1	25.1	–

Notes. The unit of observation is a $PM_{2.5}$ grid cell by month. Ever-exposed cells are grid cells crossed by at least one bus route during 2022–2024. $PM_{2.5}$ is measured in $\mu g/m^3$. Bus-kilometer variables are allocated from route-months to grid cells using route-length weights, using year-specific route geometries when available and the nearest available route geometry otherwise. The electric share is the ratio of cumulative electric bus-kilometers to cumulative total bus-kilometers.

Table A.5: Robustness to alternative exposure buffers

Dependent variable:	$PM_{2.5}$				PM_{10}				NO_x			
	1km	2km	5km	10km	1km	2km	5km	10km	1km	2km	5km	10km
	(1)	(2)	(3)	(4)	(5)	(6)	(7)	(8)	(9)	(10)	(11)	(12)
Electric bus-km nearby, 10k	-3.791	-1.801*	-0.6737**	-0.4811**	-12.22*	-3.018	-1.076*	-0.4041	-33.27*	-9.276	-3.313*	-1.181
	(2.514)	(0.8066)	(0.2499)	(0.1802)	(5.548)	(1.945)	(0.5208)	(0.3577)	(16.02)	(4.779)	(1.301)	(0.8848)
Total bus-km nearby, 10k	-0.2974	0.4388	0.2769*	0.1191**	-17.72*	-1.987	0.4267	0.1964	-9.865	6.025*	1.999***	0.6914**
	(2.451)	(1.018)	(0.1285)	(0.0426)	(8.777)	(2.109)	(0.3376)	(0.1195)	(25.18)	(2.808)	(0.2738)	(0.1745)
Station	Yes	Yes	Yes	Yes	Yes	Yes	Yes	Yes	Yes	Yes	Yes	Yes
Day	Yes	Yes	Yes	Yes	Yes	Yes	Yes	Yes	Yes	Yes	Yes	Yes
Observations	9,103	9,103	9,103	9,103	9,290	9,290	9,290	9,290	6,854	6,854	6,854	6,854

Notes. Robust standard errors are clustered at the station level. The treatment variable is electric bus-kilometers within the indicated buffer around each monitoring station, measured in units of 10,000 km. $PM_{2.5}$ and PM_{10} are measured in $\mu g/m^3$ and NO_x in parts per billion (ppb). Total nearby bus-kilometers within the same buffer are included as a control, so the coefficient on electric bus-kilometers captures changes in the composition of nearby bus service holding total bus activity fixed. Statistical significance: *** $p<0.01$, ** $p<0.05$, * $p<0.1$.

Table A.6: Robustness of noise estimates

	Workday peak	Workday off-peak	Weekend/holiday
Panel A: 50m buffer			
Baseline	-1.428***	-0.548	-0.249
	(0.437)	(0.556)	(0.352)
Station-specific linear trends	-0.385	-0.270	0.018
	(0.226)	(0.304)	(0.250)
Leave-one-station-out: minimum	-1.545	-0.750	-0.429
Leave-one-station-out: median	-1.410	-0.552	-0.252
Leave-one-station-out: maximum	0.365	0.419	0.544
Successful leave-one-station-out runs	12	12	12
Failed leave-one-station-out runs	0	0	0
Panel B: 100m buffer			
Baseline	-1.163	-0.132	-0.148
	(0.952)	(0.607)	(0.464)
Station-specific linear trends	-0.309	-0.336	-0.088
	(0.379)	(0.295)	(0.256)
Leave-one-station-out: minimum	-1.373	-0.435	-0.431
Leave-one-station-out: median	-1.166	-0.129	-0.147
Leave-one-station-out: maximum	0.795	0.475	0.531
Successful leave-one-station-out runs	12	12	12
Failed leave-one-station-out runs	0	0	0
Panel C: 200m buffer			
Baseline	-1.118	0.174	0.039
	(1.111)	(0.624)	(0.602)
Station-specific linear trends	-0.322	-0.284	-0.090
	(0.452)	(0.336)	(0.270)
Leave-one-station-out: minimum	-1.440	-0.181	-0.319
Leave-one-station-out: median	-1.147	0.175	0.044
Leave-one-station-out: maximum	0.955	0.787	0.859
Successful leave-one-station-out runs	12	12	12
Failed leave-one-station-out runs	0	0	0

Notes. The table reports robustness checks for the estimates in Table A.3. All rows report coefficients on electric bus-kilometers scaled by the mean total bus-kilometers in the corresponding buffer-period estimation sample. Thus, each coefficient is expressed in dB(A) and corresponds to replacing the average amount of nearby bus activity with electric bus activity, holding total nearby bus activity fixed. The baseline specification includes station and date fixed effects and controls for total nearby bus-kilometers, scaled in the same way. The station-trend specification additionally allows each station to follow its own linear time trend. The leave-one-station-out rows report the minimum, median, and maximum point estimates across regressions that drop one monitoring station at a time. Standard errors clustered by station are reported in parentheses for the baseline and station-trend specifications. Statistical significance: *** $p < 0.01$, ** $p < 0.05$, * $p < 0.1$.

Table A.7: Emergency-visit estimates across health-center samples

Sample	Centers treated/never	Respiratory ER visits 0–52 weeks	Respiratory ER visits >52 weeks	Non-respiratory ER visits 0–52 weeks	Non-respiratory ER visits >52 weeks	Log respiratory/non-respiratory 0–52 weeks	Log respiratory/non-respiratory >52 weeks
All centers	68; 57/11	-0.019	-0.062	-0.010	-0.064	-0.029	-0.036
		(0.029)	(0.055)	(0.023)	(0.048)	(0.044)	(0.082)
SAPU only	56; 48/8	-0.029	-0.087	-0.011	-0.068	-0.043	-0.060
		(0.034)	(0.064)	(0.029)	(0.059)	(0.051)	(0.097)
Excluding top 5 volume centers	64; 53/11	-0.005	-0.057	-0.024	-0.099	-0.014	-0.015
		(0.031)	(0.059)	(0.026)	(0.052)	(0.047)	(0.088)
Excluding top 10 volume centers	61; 51/10	-0.008	-0.062	-0.015	-0.084	-0.021	-0.027
		(0.034)	(0.066)	(0.025)	(0.053)	(0.049)	(0.092)
Excluding unstable centers	67; 56/11	-0.018	-0.045	-0.011	-0.055	-0.026	-0.031
		(0.029)	(0.053)	(0.023)	(0.047)	(0.045)	(0.085)
Excluding low-volume or unstable centers	63; 52/11	-0.014	-0.041	-0.011	-0.058	-0.015	-0.014
		(0.030)	(0.054)	(0.024)	(0.049)	(0.048)	(0.089)
Excluding top 10 or unstable centers	60; 50/10	-0.007	-0.039	-0.016	-0.072	-0.018	-0.021
		(0.034)	(0.063)	(0.025)	(0.052)	(0.050)	(0.095)
SAPU, excluding top 10 or unstable centers	51; 43/8	-0.020	-0.060	-0.014	-0.063	-0.034	-0.050
		(0.038)	(0.066)	(0.030)	(0.059)	(0.056)	(0.108)

Notes. This table reports robustness checks for the preferred emergency-visit specification. High adoption is defined as an electric share of at least 20 percent among bus-kilometers within 2 km of the health center. The omitted category is the period before high adoption, including centers that do not reach the threshold during the sample. Columns 1–4 report PPML estimates for the number of ER visits. Columns 5 and 6 report OLS estimates for the log respiratory/non-respiratory ratio. All regressions include health-center and week fixed effects. Standard errors, clustered by health center, are reported in parentheses. "Unstable centers" are centers with large changes in total ER volume between the first and last part of the sample; top-volume and low-volume restrictions are defined using average weekly ER visits.